BOUNDARY CONTROL OF FLEXIBLE BEAMS

NIPON BOONKUMKRONG

Graduate School Srinakharinwirot University

2022

การควบคุมที่ขอบของคานยืดหยุ่น

นิพนธ์ บุญคุ้มครอง

ปริญญานิพนธ์นี้เป็นส่วนหนึ่งของการศึกษาตามหลักสูตร
ปรัชญาดุษฎีบัณฑิต สาขาวิชาวิศวกรรมเครื่องกล
คณะวิศวกรรมศาสตร์ มหาวิทยาลัยศรีนครินทรวิโรฒ
ปีการศึกษา 2565

BOUNDARY CONTROL OF FLEXIBLE BEAMS

NIPON BOONKUMKRONG

A Dissertation Submitted in Partial Fulfillment of the Requirements

for the Degree of DOCTOR OF PHILOSOPHY

(Mechanical Engineering)

Faculty of Engineering, Srinakharinwirot University

2022

THE DISSERTATION TITLED

BOUNDARY CONTROL OF FLEXIBLE BEAMS

BY

NIPON BOONKUMKRONG

HAS BEEN APPROVED BY THE GRADUATE SCHOOL IN PARTIAL FULFILLMENT

OF THE REQUIREMENTS FOR THE DOCTOR OF PHILOSOPHY

IN MECHANICAL ENGINEERING AT SRINAKHARINWIROT UNIVERSITY

....

(Assoc. Prof. Dr. Chatchai Ekpanyaskul, MD.)

Dean of Graduate School

....

ORAL DEFENSE COMMITTEE

.... Major-advisor

(Asst. Prof. Dr.Pichai Asadamongkon)

.... Co-advisor

(Assoc. Prof. Dr.Sinchai Chinvorarat)

.... Chair

(Asst. Prof. Dr.Chaiyapol Thongchaisurutkul)

.... Committee

(Asst. Prof. Dr.Sommas Kaewluan)

.... Committee

(Assoc. Prof. Dr.Songkran Wiriyasart)

Title	BOUNDARY CONTROL OF FLEXIBLE BEAMS
Author	NIPON BOONKUMKRONG
Degree	DOCTOR OF PHILOSOPHY
Academic Year	2022
Thesis Advisor	Assistant Professor Dr. Pichai Asadamongkon
Co Advisor	Associate Professor Dr. Sinchai Chinvorarat

The vibration control of flexible beams is an important problem in engineering applications. Many studies have proposed that the vibration control of these beams; however, the implementation methods in practical applications are few. This dissertation investigates passivity-based boundary control for vibration suppression of flexible beams. This method incorporated an energy principle in the design, rather than a signal processing perspective. An undamped shear beam was used as a beam model, and the controller was implemented through a moving base. The storage function was defined and used to determine the control law in the design process. The finite-gain L_2 - stability of the controlled system was then proven. This technique treated the beam model PDE directly without model reduction, so control spillover was avoidable. Since the measurement and actuation in the application were non-collocated, a backstepping observer was needed for the state estimation. The controller was applied at the end of the beam via a moving base, so the beam domain was intact. This technique is readily implementable in applications. The PDE model was solved numerically using the finite-difference method. The computer simulation was used to demonstrate the performance of the controllers under the proposed control scheme. The beam vibration was suppressed satisfactorily with L_2 - stability.

Keyword : Passivity-based boundary control, Shear beam, Storage function, Backstepping observer, Vibration suppression, Partial differential equation, Finite difference equation

ACKNOWLEDGEMENTS

TABLE OF CONTENTS

LIST OF TABLES

LIST OF FIGURES

CHAPTER 1

INTRODUCTION

1.1 Background

There has been significant interest in controlling flexible beams in recent years. This interest has been motivated by the prospect of fast, light robotic arms flexing under some load. Vibration is inevitable when the robotic arm travels at a high speed. The biggest problem with task completion is this vibration. In many cases, the only practical solution to this vibration is to slow down the robotic arm or wait until the vibration has subsided.

Distributed characters or distributed parameter systems (DPS) constitute the flexible beams. The state variables of the distributed parameter system are affected by spatial and temporal variations. Models of these systems are represented mathematically using partial differential equations (PDEs).

The techniques for designing a controller to reduce or control vibration in a slender Timoshenko or shear beam are proposed in this dissertation. Since the controller is only set up at the end of the beam, it has no effect on the beam's body. For the design, the full beam model of the PDE is used, with no simplifications or approximations. Then, we can prevent the spillover problems (Boonkumkrong, Chinvorarat, & Asadamongkon, 2023, pp. 1-16).

The flexible beam model is a hyperbolic-like system that oscillates at a high frequency. As a result, high frequencies have an effect on the overall system dynamics. Spillovers cause the failure of many control system designs based on reduced or truncated finite-dimensional models that disregard the impact of high modes. In contrast to its parabolic counterpart, such as the heat equation, the dynamics of the system depends only on the first few modes; therefore, the impacts of higher modes may be minimal. Therefore, control designs using these finite-dimensional models with reduced dimensions are always insufficient.

The proposed controller in this research is designed by using passivity properties of the beam model such as dissipation, storage function etc. This method

deals directly with the system's original PDEs without the truncation of the model, so the spillover phenomenon caused by ignoring high-frequency modes is avoided.

State estimation is performed using *the backstepping observer*, a Lünberger-like observer. This observer is infinite-dimensional, which mimics the finite-dimensional one. The form of the observer is a partial differential equation (PDE). The non-collocation configuration is used for the control scheme. The proposed method of control is simple to implement in a wide variety of applications.

1.2 Objectives of the Study

Using the energy concept (the passivity property) to design the boundary control scheme for the flexible beam vibration's suppression.

1.3 Significance of the study

1. Designing a control law relies on the energy concept rather than signal processing.

2. Control spillover can be omitted because the higher modes are not removed when the system's original partial differential equation (PDE) is solved directly, with no model reduction or approximation.

3. The control technique is implemented using distributed parameter systems (of infinite dimension) rather than lumped parameter systems (of finite dimension). Natural systems are modeled using distributed parameter systems.

4. The control setup consists of non-collocated sensing and actuation, where the sensing and the actuation are placed at different locations. This configuration is simple to use in practical applications.

5. The beam body or domain remains intact since both the controller and the observer are situated at the ends of the beam.

6. The first time that the passivity-based controller is implemented with the backstepping observer.

7. The beam model is a second-order partial differential equation with an integration term, making it easy to solve numerically.

1.4 Scope of the study

1. Design the passivity-based control controller using the energy principle. First, the storage function is defined and employed to derive the control law.

2. The suitable observer is selected and incorporated into the control system. In this dissertation, the backstepping observer is used.

3. The feedback control system's stability is established, and observer convergence is presented.

4. By using finite difference equation method, partial differential equations can be numerically solved.

5. The controlled systems with and without the observer are simulated and the results are discussed.

6 The control parameters of the controller and the observer are changed, and the effects on the performance are studied.

1.5 Definition of terms

1. Partial differential equation (PDE) - a differential equation that comprises unknown functions of several variables and their partial derivatives.

2. Passive system - a system that consumes but does not produce energy. Examples are mass, spring and damper.

3. Passivity-based control – a control scheme designed by using the passivity properties of the system such as dissipation, storage function etc.

4. Lyapunov's direct method - the effective method for analyzing nonlinear and time-varying systems and a requisite for stability analysis and control law formulation. The differential equation on the system is not necessary to solve. Instead, a so-called Lyapunov function is constructed to check the stability.

5. State observer - a system that estimates the internal state of a system based on input measurements.

6. Storage function - a positively semi-definite, continuously differentiable function of the system state.

7. Non-collocated configuration – the control setup in which actuation is performed at one end and sensing is applied at the other.

8. Collocated configuration – the control setup in which the actuation and the sensing are applied at the same location.

CHAPTER 2

REVIEW OF THE LITERATURE

In this chapter, the literature pertaining the boundary controls is reviewed. The mathematical descriptions are shown as necessary. The sections are structured as follows: The developments of boundary control and distributed parameter systems, including the derivations of engineering beams, are introduced in Section 2.1. The relevant papers related to parabolic systems, which are the counterpart of hyperbolic systems, are discussed in Section 2.2. The papers on the control of hyperbolic systems such as string and wave equations are reviewed in Section 2.3, and the controls of the hyperbolic-like beam model are in Section 2.4. Section 2.5 demonstrates several applications of the boundary control, whereas Section 2.6 contains the chapter's conclusion.

2.1 Introduction

In this section, some background and information necessary for this research are investigated briefly.

Irena Lasiecka (Lasiecka, 1995, pp. 2792–2796), discussed the evolution of the control of distributed parameter systems, including string and beam systems, across time. These systems correspond to natural physical systems and are governed by partial differential equations. Physically attractive and theoretically challenging topics involving boundary and point controls are the subject of this research. However, several important results are still dispersed across the research literature. These results need a more orderly presentation.

Han R. et al. (Han, Benaroya, & Wei, 1999, pp. 935-988) developed and analyzed four engineering beams, namely the conventional Euler-Bernoulli and shear beams, which are thin beams, and the Rayleigh and Timoshenko beams, which are thick beams. The paper also presented the development history of each beam and the derivations of the beam models. For the boundary conditions, the beam frequency

equations were expressed. Using normalized wave numbers, the roots of frequency equations are expressed.

In this dissertation, the boundary control with *the backstepping observer* of the shear beam is considered.

Engineering beams mentioned above are of distributed parameter and infinite-dimensional systems expressed by partial differential equations (PDEs). Padhi R. and Ali SF. (Padhi & Ali, 2009, pp. 59–68), in their review paper, from a great deal of the literature on distributed parameter systems, the attempt was made to offer a concise description of the development in the control of the distributed parameter systems. The presentation was in chronological order. The mathematical descriptions have been omitted so a broad audience can access the paper's content.

2.2 Parabolic systems

Some papers on parabolic systems, the counterpart of hyperbolic ones, are presented in this section. The system model, such heat system, is of the first-order-in-time and second-order-in-space PDE. For the parabolic system, the first few modes of the model determine the system performance so that the higher modes can be disregarded. As compared with the hyperbolic system, the parabolic system is not difficult to control.

The issue of boundary control for the the following heat equation,

$$u_t(x,t) \quad = u_{xx}(x,t) + a(x)u(x,t), \tag{2.1}$$

was studied by WJ. Liu (Jiu, 2003, pp. 1033-1043). This equation can be made unstable by the term au with $a>0$. If $a(x)$ is a continuously differentiable function and λ is a positive constant, it can be shown in this paper that a boundary feedback control law can be formulated analytically. At a rate of λ, the system with this control scheme converges to zero exponentially.

Andrey Smyshlyaev examined the boundary stabilization of the one-dimensional parabolic partial differential equations using the backstepping technique

(Smyshlyaev & Krstic, 2004, pp. 2185-2202). Using coordinate integral transformation, the original system was changed into the known stable system. In doing so, the hyperbolic-type gain kernel PDEs, $k(x, y)$ were formulated as follows,

$$k_{xx}(x, y) - k_{yy}(x, y) = \lambda k(x, y), \tag{2.2}$$

$$k(x,0) = 0, \tag{2.3}$$

$$k(x,x) = -\frac{\lambda}{2}x. \tag{2.4}$$

The solution to the gain kernel (2.2) – (2.4) can be stated analytically as follows,

$$k(x, y) = -\lambda y \frac{I_1(x^2 - y^2)}{\sqrt{\lambda(x^2 - y^2)}}, \tag{2.5}$$

where I_1 is the 1st- order modified Bessel function of the first kind.

The gain kernel of order one is plotted for several values of λ, as shown in Figure 1.
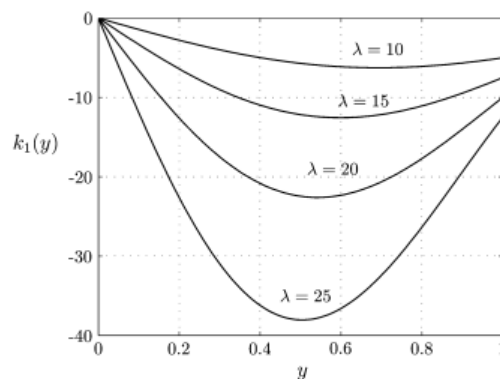
FIGURE 1 Gain kernel plot.

The controller was expressed with the gain kernel in this way,

$$u(1) = -\int_0^1 \lambda \, y \, \frac{I_1(x^2 - y^2)}{\sqrt{\lambda(x^2 - y^2)}} \, u(y) \, dy. \qquad (2.6)$$

For parabolic partial integro-differential equations, Smyshlyaev A. et al. (Smyshlyaev & Krstic, 2005, pp. 613-625) proposed the design of exponentially convergent observers. The observer error system was transformed into a target system, which was known to be exponentially stable, by using an invertible coordinate transformation. The observer gain was in closed form. The output feedback controls were in both the collocated and non-collocated sensing and the actuation setup.

Boonkumkrong N. et al. (Boonkumkrong & Kuntanapreeda, 2014, pp. 295-302) investigated the backstepping boundary control to regulate the temperature of a copper rod. At one end, a Dirichlet boundary condition was established, and at the other, a Neumann boundary condition was constructed. The rod that had a built-in heat source acted as an unstable system. The control setup was non-collocated, i.e., the sensor was at one end, and the actuation was at the opposite end. The experiment was conducted with the thermoelectric cooler acting as the controller, see Figure 2. The control scheme was evaluated by comparing the simulation and the experiment results.
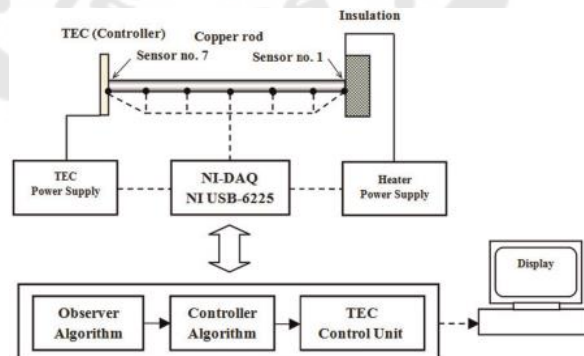
FIGURE 2 The experiment diagram.

2.3 String and Wave equations

A partial differential equation (PDE) can be used to model the hyperbolic systems of strings and waves. The model is a PDE with second-order derivative terms in both time and space. The boundary control can be applied in this kind of system model.

In 2007, Krstic et al. (Krstic, Siranosian, Balogh, & Guo, 2007, pp. 882-887) presented a backstepping boundary control scheme for the hyperbolic PDE system's controller and observer, i.e., the undamped vibrating string and a flexible beam. This design technique was also used for the vibration control of the shear and Timoshenko beams which will be discussed later. And also, in 2007 (Krstic, Guo, Balogh, & Smyshlyaev, 2007, pp. 2048-2053) and 2008 (M. Krstic, B.-Z. Guo, A. Balogh, & A. Smyshlyaev, 2008a, pp. 63-74), the issue of one-dimensional wave equation stabilization was considered by the same authors. The instability was at the free end, and the control was placed at the opposite. Using backstepping approaches, the gain kernel PDEs of the controller and observer were designed. The solution's existence and uniqueness, as well as its exponential stability, were then proven. Finally, the applications were demonstrated using simulation results.

In 2010, He W. et al. (He, Ge, Hang, & Hong, 2010, pp. 2584-2589) developed the adaptive boundary controller for a vibrating string exposed to unspecified time-varying disturbances as shown in Figure 3. The string was modelled using a PDE and several ODEs. The robustness was shown by using Lyapunov's direct method. The controller was applied at the tip of the string. Using the appropriate design parameters, it has been demonstrated that the string's state converges to a neighbourhood close to zero. Simulation results were used to prove the performance of the suggested control method.
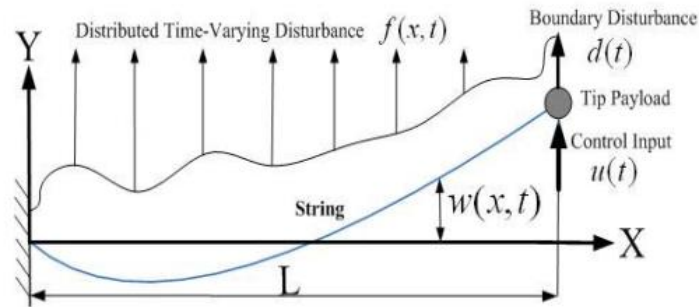
FIGURE 3 A typical string system.

In 2014, He W. et al. (He, Zhang, & Ge, 2014, pp. 1088-1093), the vibration suppression for a flexible string in both lateral and axial directions was investigated as shown in Figure 4. The governing equation of the nonlinear string was represented by two PDEs and four ODEs using Hamilton's principle for the derivation. An adaptive boundary controller was created employing Lyapunov's function. The adaptive law compensated for the parametric uncertainties. The effectiveness of the presented control law was confirmed by doing simulations on a computer.
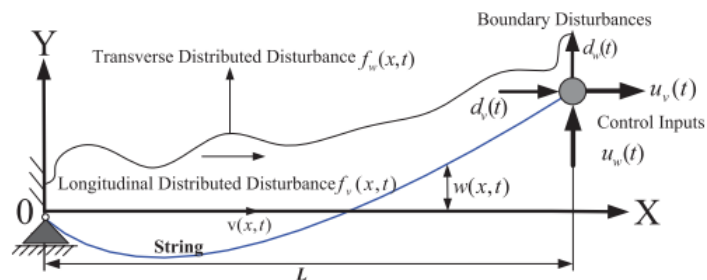
FIGURE 4 Nonlinear flexible string system.

In 2018, Zhao Z. et al. (Zhao, Liu, & Luo, 2018, pp. 323-331) studied control issue for a vibrating string system with limited input and external disturbance. The control scheme stabilized the string system globally and compensated for the input saturation effect. The disturbance observer was designed for tracking the external

disturbance. By using LaSalle's invariance concept, it was able to demonstrate asymptotic stability.

2.4 Beam equations

The engineering beam models used in the analysis include Euler-Bernoulli, shear, Rayleigh and Timoshenko beams. There are many control methodologies for controlling these beam models, such as backstepping boundary control, passivity-based boundary control, the sliding mode control etc. The beam model is represented by a fourth-order in space and a second-order in time PDE. The beam model is a hyperbolic-like system with a high-frequency oscillation character. High frequencies have effects and affect the overall system dynamics. Spillovers cause the failure of many control system designs based on reduced or truncated finite-dimensional models that neglect the impact of high modes.

2.4.1 Euler-Bernoulli beam

Euler-Bernoulli beams are the conventional engineering beams widely used in the analysis. This beam model is the simplest among the four engineering beams. Boundary control can be applied in this type of beam with various successes.

In 1992, Morgul O. (Morgul, 1992a, pp. 639-642) consider the cantilevered Euler-Bernoulli beam. At which the free end, the boundary force, and torque controls were applied. To establish stability, the energy-based Lyapunov functional of the beam system was developed. The beam vibration was satisfactorily reduced.

The control of one link flexible robot arms using direct strain feedback was investigated by Luo ZH. (Luo, 1993, pp. 1610-1622). The A-dependent operators was used for proving the closed-loop stability, the existence and uniqueness. In addition, control experiments were conducted to verify the methodology.

Two years later, Luo ZH. et al. (Luo, Kitamura, & Guo, 1995, pp. 760–765) applied direct strain feedback for vibration suppression of the SCARA-type robot with rotational joints. Both trajectory tracking control and set point control experiments were

conducted. The simple PI (Proportional and integration) plus shear force feedback could help with both the movement of the robot arm and the damping of vibrations.

In 2002, Fard MP. (Fard, 2002, pp. 239-258), the Lagrangian equations for distributed-parameter mechanical systems using Hamilton's principle were developed and then used for nonlinear Euler-Bernoulli beam model derivation. The passivity property of the system was employed for controller design. The resulted controller was in the form of mass, damping and spring forces as shown in Figure 5. The feedback control system was shown to have finite gain L_2 − stability. Finally, simulation results were demonstrated to show the controller's performance.
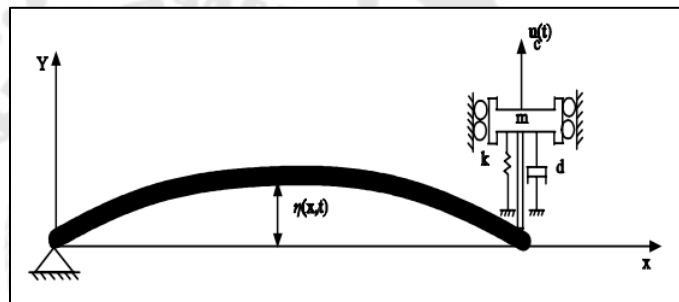
FIGURE 5 A vibrating beam with a MDS boundary controller.

Smyshlyaev et al. in 2008 (Smyshlyaev, Guo, & Krstic, 2008, pp. 185-190), the stability of the Euler-Bernoulli beam was investigated. Figure 6 depicts the left boundary as a sliding end while the right boundary was actuated by displacement and moment.

FIGURE 6 The Euler-Bernoulli beam with the sliding and pivoting ends.

A year later, in 2009, the Euler-Bernoulli Beam which was expressed in the Schrodinger equation (Smyshlyaev, Guo, & Krstic, 2009, pp. 1134-1140) was controlled using the backstepping boundary control technique. The integral transformation transformed the resulting equation into a target system that is exponentially stable. The control method's efficacy was shown through simulations.

The suppression of the beam, which was pinned at one end and the controlled sliding end, was investigated by Guo et al. (Guo & Jin, 2010, pp. 2098–2106). Before any design could be made, the Euler-Bernoulli beam had to be stated as a coupled heat-like equation. The backstepping technique might be put into practice by using this process. Then, an exponential target system with a specified decay rate was substituted for the original beam model. Unlike Smyshlyaev et al. (Smyshlyaev et al., 2009, pp. 1134-1140), there are no limitations on which boundary control problems may be applied using this method.

An unknown disturbance was assumed to be affecting the control of the beam's vibration, Figure 7, and Ge SS et al. (Ge, Zhang, & He, 2011, pp. 2988-2993) used Hamilton's concept to develop the adaptive boundary control. The beam's end was where the controller was put into action. It was shown that the beam state tends to approach zero. Simulation results demonstrated the controller's effectiveness.
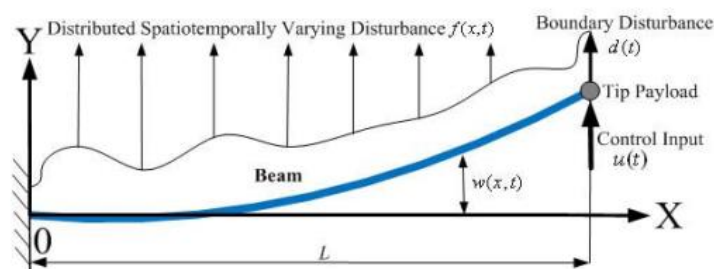
FIGURE 7 A typical Euler-Bernoulli Beam.

In 2018, Liu Z et al. (Z. Liu, Liu, & He, 2018, pp. 531–541) studied the control technique for the conventional Euler–Bernoulli beam, whose input and output

were both bounded and which was exposed to disturbances. A boundary control scheme for damping vibrations was developed using the backstepping method. The partial differential equations of the system were treated directly. An auxiliary system was designed to manage the impact of the restricted input, and a Lyapunov function was implemented to reduce the effects of output restriction. Simulation results verified the effectiveness of the control scheme.

2.4.2 Shear and Rayleigh beams

The shear and Rayleigh beam models are more complex than the Euler-Bernoulli beam. The shear beam has an additional shear deformation term in the model. In the case of the Rayleigh beam, the rotating inertia term is included. Shear and Rayleigh beams are mathematically similar but physically different. The shear beam is a thin beam, but the Rayleigh beam is a thick beam. In this thesis, the shear beam model is studied.

In 2003, Krener et al. (Krener & Kang, 2003, pp. 155-177) proposed a new method for designing the observer for nonlinear systems using a backstepping technique. This work was the motivation for Krstic's later works. The designed observer was globally convergent. As a result, the estimated error between the full-state plant and the observer decayed to zero exponentially.

In 2006, Krstic et al. (Krstic, Balogh, & Smyshlyaev, 2006a, pp. 1389-1394), the undamped shear beam's control was examined. The beam was set up in a cantilevered configuration. The novel control strategy integrated the backstepping boundary control method with the damping boundary feedback method. The original unstable beam was transformed into the stable boundary-damped wave equation. The coordinate integral transformation was used to change this variable,

$$w(x) = u(x) - \int_0^1 k(x, y) u(y) \, dy, \qquad (2.7)$$

where $u(x,t)$ is the variable of the original system and $w(x,t)$ is the variable of the target system. The control setup was the non-collocated measurement and actuation, which was easily implementable in many applications. The measurement was done at the free end of the beam, while the opposite end was utilized to implement the boundary feedback controller as follows,

$$u_x(1) = k(1,1)\,u(1) + \int_0^1 k_x(1,y)\,u(y)\,dy \qquad (2.8)$$

$$-c_1\,u_t(1) + c_1\int_0^1 k(1,y)\,u_t(y)\,dy,$$

where

$u(x,t)$ is the lateral displacement,

$k(x,y)$ is the gain kernel of the beam.

When the piezo-actuator was used at the base of the beam, this technique can be used for an atomic force microscopy (AFM). The observer design for state estimation was done with a similar technique. The design parameters were easily selected to achieve the desired performance.

In 2018, Boonkumkrong et al. (Boonkumkrong, Chinvorarat, & Asadamongkon, 2018, pp. 1-11), the vibration of the beam, which was attached to the moving base, was eliminated by using boundary control.

Using a passivity-based boundary controller with a moving base, (Boonkumkrong et al., 2023, pp. 1-16), the vibrations of the flexible beam can be suppressed. The control designs might be classified as collocational or anti-collocational, whether the beam's actuation and sensing were situated at the same or opposite ends. With the latter, estimating the state required the use of the backstepping observer. The controller was a PD-style controller. The control results were satisfactory.

Liu JJ et al. studied the stabilization of a shear beam's tip force subjected to disturbance matched boundary control (J. J. Liu, Chen, & Wang, 2016, pp. 117-128). To

regulate the unknown bounded external disturbance, the sliding mode control (SMC) was used. Finally, the closed-loop system solution's existence and uniqueness were established.

Lertphinyovong J. et al. (Lertphinyovong & Khovidhungij, 2008, pp. 8731–8736), the Rayleigh beam was controlled using the backstepping boundary control. The original system was transformed into an exponentially stable system using a backstepping-like integral transformation. In doing so, the backstepping controller was formulated. The measurement and actuation were non-collocated in the control setup. The same technique was applied for the observer designs. Using simulation results, the performance of the closed-loop system is verified.

2.4.3 Timoshenko beam

Among the four engineering beams, the Timoshenko beam model is the most advanced. Both shear deformation and rotational inertia are included in the conventional Euler-Bernoulli beam. The boundary feedback controller is also used to control the Timoshenko beam.

The boundary control of Timoshenko beams was investigated by Kim JU. and Renardy Y. (Kim & Renardy, 1987, pp. 1417-1429). The function of the energy stored in the beam and a moving base system is described by

$$\varepsilon(t) = \frac{1}{2} \int_0^L \left\{ \rho\,(\frac{\partial w}{\partial t})^2 + I_\rho(\frac{\partial \phi}{\partial t})^2 + K\,(\phi - \frac{\partial w}{\partial x})^2 + EI\,(\frac{\partial \phi}{\partial x})^2 \right\} dx, \qquad (2.9)$$

where

$w(x,t)$ is the lateral displacement.

$\phi(x,t)$ is the rotation angle of the beam subject to pure bending.

ρ is the mass per unit length

I_ρ is the mass moment of inertia of the area.

I is the moment of inertia of the area.

E is Young's modulus.

For the shearing term, the coefficient K is equal to kGA, where G is the modulus of elasticity in shear, A is the cross-sectional area and k is a shape factor. The boundary control mechanism was in the form of lateral force and moment applied at the beam end. This energy equation will be modified for the controller design in this thesis.

Morgul (Morgul, 1992b, pp. 1255-1260) also applied the same methodology as the Euler-Bernoulli beam case mentioned above to control the more advanced Timoshenko beam. The beam's vibration was exponentially and uniformly reduced to zero.

The passivity and direct feedback control law for flexible mechanical systems were studied by Matsuno F. and Murata K. in 1999 (Matsuno & Murata, 1999, pp. 51-56). The Lyapunov function of the system was introduced and used to derive the control law. Asymptotic stability was proven using the differential operator and the invariance principle. Lastly, experiments were carried out in order to validate the effectiveness of the proposed control strategy.

In 2006, it was proposed in two separate articles that the Timoshenko beam's vibration may be suppressed by using a backstepping boundary control technique. Part one was the design methodology (Krstic, Siranosian, & Smyshlyaev, 2006, pp. 2412–2417), and part two was the stability analysis and simulations (Krstic, Siranosian, Smyshlyaev, & Bement, 2006, pp. 3938-3943). Shear deformation and rotational inertia were considered in the Timoshenko beam model. In Figure 8, the beam element was displayed.
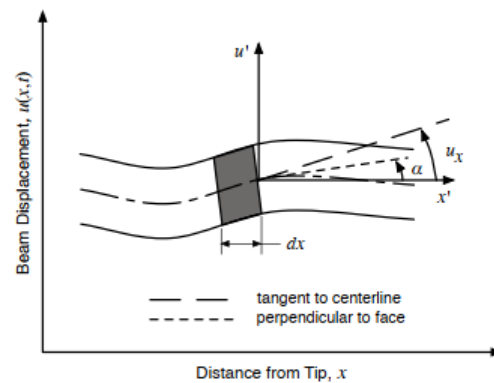
FIGURE 8 The beam element.

In the beam model, a small amount of Kelvin-Voigt damping was permitted. This damping was the internal friction present in the real material. The designs of the controller and the observer were the same as in the case of the undamped shear beam that was previously mentioned. The unstable beam was converted to the stable target system (a wave equation with a damping boundary) using the coordinate integral transformation, and the process is shown in Figure 9.
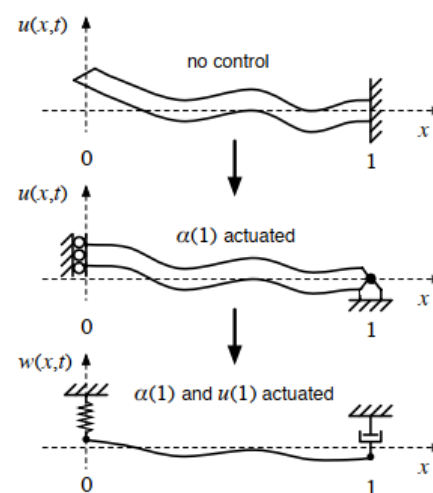
FIGURE 9 Beam behavior with various steps of control.

The measurement and actuation were not collocated in the control configuration. In the mathematical solving of the Timoshenko beam model, the singularly perturbed approximation was used to reduce the original beam into the shear beam model and solved for the system response.

In 2012, Sasaki M. et al. (Sasaki, Ueda, Inoue, & Book, 2012, pp. 1-6) investigated the controls of translational and rotational Timoshenko robotic arms. For controller design, the beam's passivity property was used. Without using a model approximation, it directly dealt with the PDE of the beam system. The stability of the feedback control was proven in $L_2 - $ sense. The performance of the proposed controller was found to be effective.

In the same year, the authors also investigated methods for suppressing vibrations in a rotational arm, Figure 10 (Sasaki, Shimizu, Inoue, & Book, 2012, pp. 1-7). The control scheme consisted of a gain tuning with the neural network and a variable gain feedback control. The neural network learned the optimal gain of the controller. Lyapunov's direct method was used in the process of developing the controller. The presented controller was effective in vibration suppression.
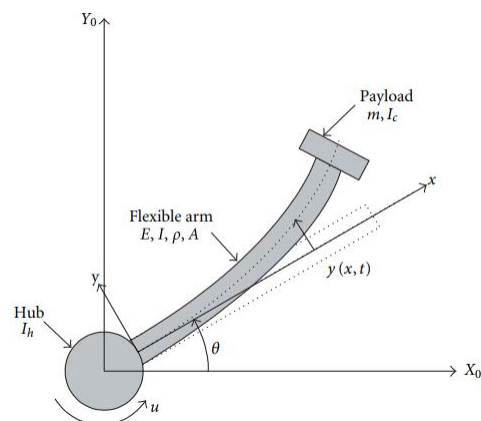
FIGURE 10 A Rotational flexible arm.

In the paper of Zhao Z. and Liu Z. (Zhao & Liu, 2021, pp. 157-168), for a Timoshenko manipulator that was affected by a convergence disturbance-removing

scheme was designed. In a limited period of time, the estimation error was reduced to zero in a limited period of time.

2.5 Some applications of the boundary control

The boundary control can be implemented in many applications. In this section, some papers on the boundary control applications are presented.

In 2013, He W. et al. (He, Zhang, & Ge, 2013, pp. 5802-5810) investigated the control problem of the marine riser installation, which consists of a vessel, a flexible riser to be installed, and the payload under the sea in Figure 11. The system's adaptive boundary control was made with the help of a Lyapunov direct technique. The proposed control scheme was used to locate the payload in the desired position and to suppress the vibration of the riser. The controllers were placed at the top and the bottom of the riser. The design parameters were chosen for the desired performance. The control technique was shown to be successful via simulation.
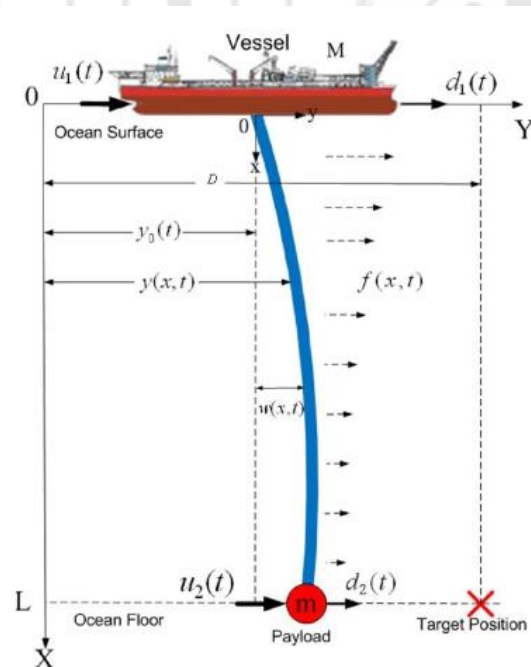
FIGURE 11 Typical beam-like marine riser installation system.

In 2014, He W. et al. (He, Sun, & Ge, 2014, pp. 497-505) analyzed the technique of boundary control for reducing vibrations in a maritime riser pipe. The flexible riser was described by the PDEs. The boundary controller, which located at the top of the riser, was designed using the integral-barrier Lyapunov function to suppress the riser vibration. Because of the existence of the parametric uncertainty, the authors the designed an adaptive controller to cope with this situation. The stability study was carried out with Lyapunov's theory of stability. Simulation results demonstrated the effectiveness of the control schemes.

Liu Y. et al. (Y. Liu, Fu, He, & Hui, 2018, pp. 8648–8658). considered spacecraft's flexible structure subject to external disturbances. An observer-based control was developed to remove vibration and maintain the proper orientation. An infinite-dimensional disturbance observer was utilized to decrease the disturbance. It has been shown that the developed control system is stable.

Liu Y. et al. (Y. Liu, Chen, Wu, Cai, & Yokoi, 2021, pp. 1-9) analyzed the angle control and vibration suppression of a spacecraft. The adaptive neural network control was developed via backstepping and Lyapunov's direct technique. A barrier Lyapunov was applied to guarantee that the angle tracking error remained within the acceptable limit. Lyapunov analysis was used to demonstrate that the feedback control system was stable.

2.6 Chapter conclusion

This chapter reviewed the literature concerning boundary control and the related issues. The boundary control of the parabolic such as heat system, hyperbolic such as string system or wave equation, hyperbolic-like such as beam models, is considered.

The parabolic system model is the first-order-in-time and second-order-in-space PDE. The heat system model is a parabolic. For the parabolic systems, the first few modes of the model determine the system performance so that the higher modes can be disregarded. So, the parabolic systems were easy to control compared to their hyperbolic counterpart.

The boundary control was also applied successfully to control the hyperbolic systems such as string, wave equations and other mechanical systems.

The flexible beam model is a hyperbolic-like system that oscillates at a high frequency. As a result, high frequencies have an effect on the overall system dynamics. Spillovers cause the failure of many control system designs based on reduced or truncated finite-dimensional models that disregard the impact of high modes. All engineering beam theories, including Euler-Bernoulli, shear, Rayleigh, and Timoshenko beams, are suitable for boundary control.

For the controller and observer stability proof, there were many techniques used such as Lyapunov's direct method, passivity property, the invariance principle etc.

Both collocated and non-collocated configulations can be used depended on in the location of the actuation and sensing, and also based on the design techniques of each methodology. For the non-collocated configulation, in which the sensing and actuation were placed in opposition to one another, it is easier to implement in practical applications.

The feedback boundary control technique was employed in many applications such as atom force microscopy (AFM), marine riser installation, container crane control, space structure etc.

CHAPTER 3
METHODOLOGY

This chapter presents the mathematical fundamentals and theories for designing the passivity-based controller. The engineering beam models, such as shear, and Timoshenko beams, etc., are derived in Section 3.1. The passivity property of the beams and some lemmas are explained in Section 3.2. In Section 3.3, the passivity-based control design technique is demonstrated. Section 3.4 demonstrates the backstepping observer technique for state estimation, and Section 3.5 contains the chapter's conclusion.

3.1 Derivation of Engineering beam models

The beam model in engineering applications consists of the following four models: the Timoshenko, shear, Rayleigh, and Euler-Bernoulli beams. The Euler-Bernoulli beam is the most commonly employed fundamental beam model. For this beam, the effects of beam displacement and bending moment are considered. The Euler-Bernoulli beam is turned into the Rayleigh beam by adding the rotating inertia term. Similarly, with shear deformation applied to the Euler-Bernoulli beam, the beam model changes into the shear beam. Mathematically, the equation of motion of the Rayleigh and shear beams is the same, but only the parameter of a specific term is different. In Timoshenko beam theory or thick beam theory, the effects of beam displacement, bending moment, rotary inertia, and shear deformation are all incorporated.

Consider the beam element is shown in Figure 12 (Rao, 2011, pp. 699-768). If the shear deformation is disregarded, the tangent to the deflected center line will coincide with the normal to the element's face. The tangent to the deformed center line cannot be perpendicular to the face due to shear deformation. The amount of shear deformation can be determined by the angle that exists between the normal to the face and the tangent to the deformed center line.
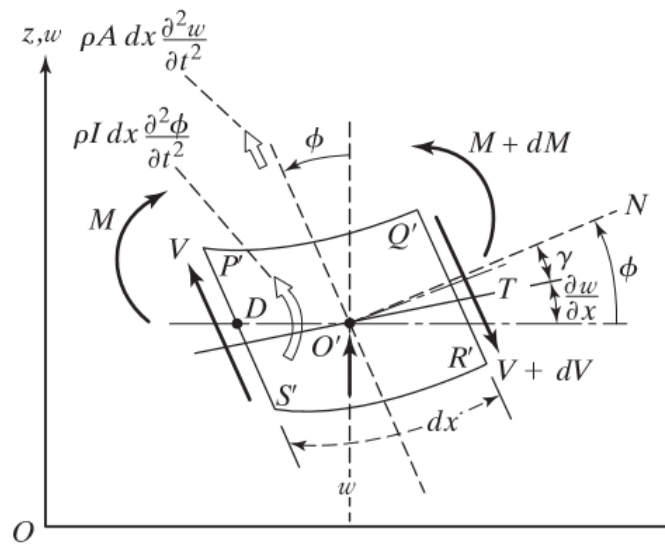
FIGURE 12 An element of Timoshenko beam.

In Figure 12, notice that the positive shear acting downward on the element's right face. The shear deformation is expressed as following,

$$\gamma = \phi - \frac{\partial w}{\partial x}, \tag{3.1}$$

where ϕ is the slope of the deflection line due to pure bending alone

Note also that the element undergoes distortion alone but not rotation because of shear.

According to the mechanics of solids, the bending moment M and shear force V related to ϕ and w as follows,

$$M = EI \frac{\partial \phi}{\partial x}, \tag{3.2}$$

$$V = k\,AG\gamma = k\,AG\left(\phi - \frac{\partial w}{\partial x}\right), \tag{3.3}$$

where

G is the modulus of rigidity of the beam's material

k is Timoshenko's shear coefficient.

The value of k is $9/10$ for a circular section and $5/6$ for a rectangular section.

From Hooke's law, $\tau = G\gamma$, note also that

$$V = \tau A = \gamma GA. \tag{3.4}$$

For each of the different cross-sectional shapes, the right-hand side of this equation is modified by a factor k, as mentioned above, resulting in the equation becoming $V = kGA\gamma$.

Using Newton's second law, we can derive the motion equation for the element in Figure 12:

In the z direction, the translation of the element is as follows,

$$-[V+dV] + f\,dx + V = \rho A\,dx\frac{\partial^2 w}{\partial t^2}. \tag{3.5}$$

For the rotation about a line parallel to the y-axis and passing through point D:

$$[M+dM] + [V+dV]\,dx + f\,dx\frac{dx}{2} - M = \rho I\frac{\partial^2 \phi}{\partial t^2}. \tag{3.6}$$

Using the relations $dV = \dfrac{\partial V}{\partial x}dx$ and $dM = \dfrac{\partial M}{\partial x}dx$ along with Eq. (3.2) and (3.3) and disregarding terms involving second powers in dx, Eq. (3.5) and (3.6) can be expressed as

$$-kAG\left(\frac{\partial \phi}{\partial x} - \frac{\partial^2 w}{\partial x^2}\right) + f = \rho A\frac{\partial^2 w}{\partial t^2}, \tag{3.7}$$

$$EI\frac{\partial^2\phi}{\partial x^2} - kAG\left(\phi - \frac{\partial w}{\partial x}\right) = \rho I\frac{\partial^2\phi}{\partial t^2}. \tag{3.8}$$

Solving Eq. (3.7) for $\partial\phi/\partial x$,

$$\frac{\partial\phi}{\partial x} = -\frac{\rho A}{kAG}\frac{\partial^2 w}{\partial t^2} + \frac{f}{kAG} + \frac{\partial^2 w}{\partial x^2}. \tag{3.9}$$

Substituting the above equation Eq. (3.9) into Eq. (3.8), we reach the desired equation of motion for a uniform beam's forced vibration:

$$EI\frac{\partial^4 w}{\partial x^4} + \rho A\frac{\partial^2 w}{\partial t^2} - \rho I\left(1+\frac{E}{kG}\right)\frac{\partial^4 w}{\partial x^2\partial t^2} + \frac{\rho^2 I}{kG}\frac{\partial^4 w}{\partial t^4} + \frac{EI}{kAG}\frac{\partial^2 f}{\partial x^2} \tag{3.10}$$

$$- \frac{\rho I}{kAG}\frac{\partial^2 f}{\partial t^2} - f = 0.$$

The equation (3.10) is called *the Timoshenko beam*.

For free vibration, $f = 0$ and Eq. (3.10) becomes

$$EI\frac{\partial^4 w}{\partial x^4} + \rho A\frac{\partial^2 w}{\partial t^2} - \rho I\left(1+\frac{E}{kG}\right)\frac{\partial^4 w}{\partial x^2\partial t^2} + \frac{\rho^2 I}{kG}\frac{\partial^4 w}{\partial t^4} = 0. \tag{3.11}$$

For solving Equation (3.10) or Equation (3.11), the following boundary conditions might be used.

The deflection and slope of the beam are both zero for a clamped or fixed boundary.

$$w = \phi = 0. \tag{3.12}$$

For simply supported or hinged boundary, both the deflection and the bending moment are zero,

$$w = EI\frac{\partial \phi}{\partial x} = 0. \tag{3.13}$$

With a free boundary, there is no shear force and no bending moment at the end.

$$kAG\left(\frac{\partial w}{\partial x} - \phi\right) = EI\frac{\partial \phi}{\partial x} = 0. \tag{3.14}$$

No shear force and no beam slope existed for the end of the beam fixed to the moving base,

$$kAG\left(\frac{\partial w}{\partial x} - \phi\right) = \phi = 0. \tag{3.15}$$

Note that the following rotary inertia and shear deformation affect the beam model:

If only the effect of rotating inertia is taken into account, the equation of motion, Eq. (3.11), contains no terms involving the shear coefficient k.

$$EI\frac{\partial^4 w}{\partial x^4} + \rho A\frac{\partial^2 w}{\partial t^2} - \rho I\frac{\partial^4 w}{\partial x^2 \partial t^2} = 0. \tag{3.16}$$

Eq. (3.16) is called *the Rayleigh beam*.

Considering only the effect of shear deformation, the term $\rho I\,\partial^4 w \big/ \partial x^2 \partial t^2$ does not appear in the equation of motion. As a result, we obtain the motion equation,

$$EI\frac{\partial^4 w}{\partial x^4} + \rho A\frac{\partial^2 w}{\partial t^2} - \frac{EI\rho}{kG}\frac{\partial^4 w}{\partial x^2 \partial t^2} = 0. \tag{3.17}$$

Eq. (3.17) is called *the shear beam* or *slender Timoshenko beam*. A beam with a length-to-width ratio greater than 10 is considered a slender beam (Sasaki, Ueda, et al., 2012, pp. 1-6). Notice that Eq. (3.16) and (3.17) have the same structure mathematically, besides the different parameter of the term $\partial^4 w / \partial x^2 \partial t^2$.

If we ignore the effects of shear deformation and rotating inertia, Eq. (3.11) becomes

$$EI\frac{\partial^4 w}{\partial x^4} + \rho A\frac{\partial^2 w}{\partial t^2} = 0. \tag{3.18}$$

Eq. (3.18) is *the conventional Euler-Bernoulli beam*.

This research uses Eq. (3.17) as the model to be studied, which constitutes the most engineering beams used in many practical applications. From Eq. (3.7), with $f = 0$ and (3.8), the shear beam can be described as a coupled wave equation and a second-order spatial ordinary differential equation as follows,

$$-kAG\left(\frac{\partial \phi}{\partial x} - \frac{\partial^2 w}{\partial x^2}\right) = \rho A\frac{\partial^2 w}{\partial t^2}, \tag{3.19}$$

$$EI\frac{\partial^2 \phi}{\partial x^2} - kAG\left(\phi - \frac{\partial w}{\partial x}\right) = 0. \tag{3.20}$$

3.2 Passivity Property

This section aims to introduce the concept of passivity and present some of the stability results obtained using this framework. A passive component is one that consumes but does not create energy. The passive component is incapable of power gain. Examples are resistor, inductor and capacitor for electrical systems and mass, spring and damper for mechanical systems.

The so-called storage function will be used for stability analysis. We can think of the storage function as the system's internal energy. All passive systems have a stable origin. To stabilize the origin, damping is injected into the system so that energy will dissipate whenever the state is not identically zero. For a dynamic system, let us define passivity now. Consider the following state model,

$$\dot{x} = f(x, v), \tag{3.21}$$

$$y = h(x, v), \tag{3.22}$$

where

x is the state variable,

y is the output variable,

v is the input.

The function $f(x, v)$ is locally Lipschitz, and $h(x, v)$ is a continuous function, where $f(0,0) = 0$, and $h(0,0) = 0.$ There are an equal number of inputs and outputs in the system.

Notice that the variables x and y will also be used as spatial variables in the controller and observer designs.

<u>Definition 1</u> The system is said to be passive if there is a function $V(x)$ called the storage function that is a continuously differential positive semi-definite function such that, (Khalil, 2002, p. 236)

$$v^T y \geq \dot{V}. \tag{3.23}$$

<u>Lemma 1</u> If the system Eq. (3.21) – (3.22) is output strictly passive with $v^T y \geq \dot{V} + \delta\, y^T y$, for some $\delta > 0$, where v and y are input and output, respectively, then it is finite-gain $L_2 -$ stable (Khalil, 2002, p. 242).

Proof

Consider the function V of the variable x, called the storage function. This function's derivative satisfies the condition:

$$\dot{V} \leq v^T y - \delta y^T y = -\frac{1}{2\delta}(v - \delta y)^T(v - \delta y) + \frac{1}{2\delta}v^T v - \frac{\delta}{2}y^T y, \qquad (3.24)$$

$$\leq \frac{1}{2\delta}v^T v - \frac{\delta}{2}y^T y.$$

To get the result, integrate both sides over $[0, \tau]$

$$\int_0^\tau y^T(t) y(t)\, dt \leq \frac{1}{\delta^2} \int_0^\tau v^T(t) v(t)\, dt - \frac{2}{\delta} \int_0^\tau \dot{V}\, dt,$$

$$\leq \frac{1}{\delta^2} \int_0^\tau v^T(t) v(t)\, dt - \frac{2}{\delta}[V(x(\tau)) - V(x(0))]. \qquad (3.25)$$

Take the square root on both sides, we get

$$\sqrt{\int_0^\tau y^T(t) y(t)\, dt} \leq \sqrt{\frac{1}{\delta^2} \int_0^\tau v^T(t) v(t)\, dt - \frac{2}{\delta}[V(x(\tau)) - V(x(0))]}. \qquad (3.26)$$

With the fact that $V(x) \geq 0$, the inequality can be reduced to

$$\sqrt{\int_0^\tau y^T(t) y(t)\, dt} \leq \sqrt{\frac{1}{\delta^2} \int_0^\tau v^T(t) v(t)\, dt + \frac{2}{\delta}V(x(0))}. \qquad (3.27)$$

For any nonnegative numbers a and b, then $\sqrt{a^2 + b^2} \leq a + b$, we obtain

$$\sqrt{\int_0^\tau y^T(t)\,y(t)\,dt} \;\leq\; \sqrt{\frac{1}{\delta^2}\int_0^\tau v^T(t)\,v(t)\,dt} + \sqrt{\frac{2}{\delta}V(x(0))}\,. \qquad (3.28)$$

Finally, the equation is expressed as a norm notation,

$$\left\| y_\tau \right\|_{L_2} \;\leq\; \frac{1}{\delta}\left\| v_\tau \right\|_{L_2} + \sqrt{\frac{2}{\delta}\,V(x(0))}\,, \qquad (3.29)$$

where $\left\| y_\tau \right\|_{L_2}$ and $\left\| v_\tau \right\|_{L_2}$ are $L_2 -$norms. So, the lemma is proved.

Lemma 2 If the system with a positive, definite storage function $V(x)$ is passive, then the origin of $\dot{x}=f(x,0)$ is stable (Khalil, 2002, p. 242).

3.3 Design of Passivity-based Controller

This section will demonstrate the control design based on passivity. The internal energy of the beam will be used as a storage function in the control scheme's development. The finite-gain stability and passivity of the feedback system are shown further.

Usually, the shear beam (3.17) can be expressed in a short form (Krstic & Smyshlyaev, 2008, p. 91),

$$w_{tt}(x,t) \;-\; \varepsilon w_{xxtt}(x,t) \;+\; w_{xx}(x,t) \;=\; 0, \qquad (3.30)$$

where $\varepsilon > 0$ is a constant depending on the shear modulus.

The shear beam model (3.19) and (3.20) can be expressed in short forms as follows (Krstic & Smyshlyaev, 2008, p. 91),

$$\varepsilon\, w_{tt}(x,t) \;=\; w_{xx}(x,t) - \phi_x(x,t)\,, \qquad (3.31)$$

$$\phi_{xx}(x,t) - \phi(x,t) + w_x(x,t) = 0. \tag{3.32}$$

The beam models (3.30), and (3.31) – (3.32) are equivalent. We can verify this by taking the following steps (Krstic & Smyshlyaev, 2008, p. 91),

a) $(3.27)_x + (3.28) = (\#),$

b) $(\#)_x = (\#\#),$

c) $(\#\#) + \dfrac{1}{\varepsilon}(3.27) = (3.26).$

The beam model (3.31) – (3.32) is the equation that is reduced from the fourth-order equation. This form of equation will be employed for the control scheme derivation and for the numerical simulation; it is also used in the development of the finite difference equation.
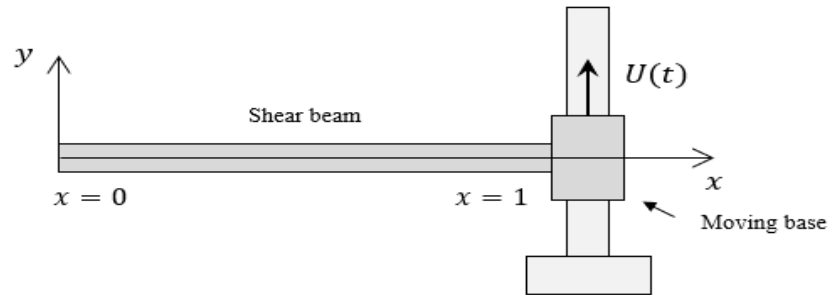
FIGURE 13 Shear beam model with the moving base.

As shown in Figure 13, the investigated beam is a cantilever-type beam, which is fixed at the base on the right and free on the left (Boonkumkrong et al., 2023, pp. 1-16). The free end has the following boundary conditions:

$$w_x(0,t) - \phi(0,t) = 0, \tag{3.33}$$

$$\phi_x(0,t) = 0. \tag{3.34}$$

As shown in Eqs. (3.33) and (3.34), the shearing force and bending moment are zero at the free end, respectively.

The boundary conditions at the moving end are

$$m\ W_{tt}(t) + [\,w_x(1,t) + \phi(1,t)\,] \ = \ U(t), \tag{3.35}$$

$$\phi(1,t) \ = \ 0, \tag{3.36}$$

$$w\ (1,t) \ = \ 1. \tag{3.37}$$

In Eq. (3.35), $U\ (t)$ is the boundary controller implemented at the end of the beam via a moving base and from Eq. (3.36) - (3.37), the slope and the deflection at are zero, respectively.

Note also that in the boundary conditions at both ends, i.e., at $x=0$ and at $x=1$ are the functions of time, t only.
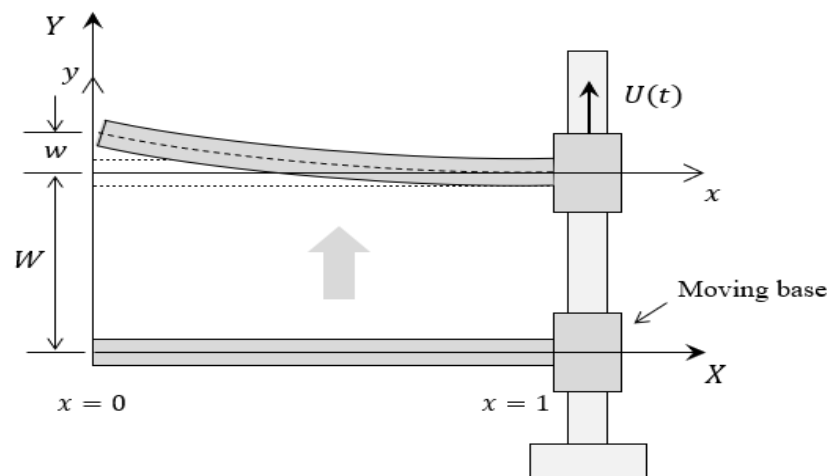
FIGURE 14 Shear beam model with coordinates

In Figure 14, the model consists of the beam sliding along the column through the moving base. In the model, there are two coordinates. The first is a global coordinate

$X - Y$ fixed to the ground, which does not move with the beam. Another is a local coordinate $x - y$ located on the beam base and moves with the beam.

For the coordinate $X - Y$, the deflection of the beam is expressed as

$$\bar{w}\,(x,t) \;=\; w\,(x,t) \;+\; W(t),\tag{3.38}$$

where $W(t)$ is the displacement of the moving base along the column and is the function of time, t only.

The beam model (3.31) – (3.32) are expressed in the global coordinate as follows,

$$\varepsilon\,\bar{w}_{tt}(x,t) \;=\; \bar{w}_{xx}(x,t) - \phi_x(x,t),\tag{3.39}$$

$$\phi_{xx}(x,t) - \phi(x,t) + \bar{w}_x(x,t) \;=\; 0.\tag{3.40}$$

Substituting Eq. (3.38) into (3.39) and (3.40)

$$\varepsilon\,[w_{tt}(x,t) + W_{tt}(t)] \;=\; w_{xx}(x,t) - \phi_x(x,t),\tag{3.41}$$

$$\phi_{xx}(x,t) + w_x(x,t) - \phi(x,t) \;=\; 0.\tag{3.42}$$

Note that $\bar{w}_x(x,t) = w_x(x,t)$ and $\bar{w}_{xx}(x,t) = w_{xx}(x,t)$

We propose the following controller which will be applied at the moving base.

$$U(t) \;=\; -c_1 W_t(t) + v(t),\tag{3.43}$$

where the constant c_1 is positive. On the right-side of the equation, the first term is a damping force, and the variable $v(t)$ is a control element that will be determined in the next step.

In this study, the internal energy of the beam and the moving base will be used to define the following storage function: (Boonkumkrong et al., 2023, pp. 1-16),

$$V(t) = \frac{1}{2} \int_0^1 \varepsilon \, [\, w_t(x,t) \, + \, W_t(t) \,]^2 \, dx \qquad (3.44)$$

$$+ \frac{1}{2} \int_0^1 \phi_x^2(x,t) \, dx \, + \frac{1}{2} \int_0^1 [\, \phi(x,t) - w_x(x,t) \,]^2 dx + \frac{1}{2} m W_t^2(t).$$

The above function represents the potential and kinetic energies of the beam and the moving base. The first right-hand integral represents kinetic energy. The strain (potential) energies are represented by the second and third integrals. The last term stands for the moving base's kinetic energy.

The time rate of change of the storage function (3.44) is as follows,

$$\dot{V}(t) = \int_0^1 \varepsilon \, [\, w_t(x,t) + W_t(t) \,] \, [\, w_{tt}(x,t) + W_{tt}(t) \,] \, dx \qquad (3.45)$$

$$+ \int_0^1 \phi_x(x,t) \, \phi_{xt}(x,t) \, dx$$

$$+ \int_0^1 [\, \phi(x,t) - w_x(x,t) \,] [\, \phi_t(x,t) - w_{xt}(x,t) \,] \, dx \, + \, m W_t(t) W_{tt}(t).$$

Substituting Eq. (3.41) into the first integral term of Eq. (3.45), yields

$$\dot{V}(t) = \int_0^1 [\, w_t(x,t) + W_t(t) \,] [\, w_{xx}(x,t) - \phi_x(x,t) \,] \, dx \qquad (3.46)$$

$$+ \int_0^1 \phi_x(x,t) \phi_{xt}(x,t) \, dx$$

$$+ \int_0^1 [\, \phi(x,t) - w_x(x,t) \,] [\, \phi_t(x,t) - w_{xt}(x,t) \,] \, dx + m W_t(t) W_{tt}(t).$$

The square brackets in the integrands of the first and last integrals are multiplied, so the equation becomes,

$$\dot{V}(t) = \int_0^1 w_t(x,t)[w_{xx}(x,t) - \phi_x(x,t)]\,dx \tag{3.47}$$

$$+ W_t(t)\int_0^1 [w_{xx}(x,t) - \phi_x(x,t)]\,dx + \int_0^1 \phi_x(x,t)\phi_{xt}(x,t)\,dx$$

$$+ \int_0^1 \phi_t(x,t)[\phi(x,t) - w_x(x,t)]\,dx$$

$$- \int_0^1 w_{xt}(x,t)[\phi(x,t) - w_x(x,t)]\,dx + mW_t(t)W_{tt}(t).$$

Integrating the second term and integrating by parts the third and fifth terms, we obtain,

$$\dot{V}(t) = \int_0^1 w_t(x,t)[w_{xx}(x,t) - \phi_x(x,t)]\,dx \tag{3.48}$$

$$+ W_t(t)[w_x(1,t) - \phi(1,t)] - W_t(t)[w_x(0,t) - \phi(0,t)]$$

$$+ \phi_x(1,t)\phi_t(1,t) - \phi_x(0,t)\phi_t(0,t) - \int_0^1 \phi_{xx}(x,t)\phi_t(x,t)\,dx$$

$$+ \int_0^1 \phi_t(x,t)[\phi(1,t) - w_x(x,t)]\,dx$$

$$- w_t(1,t)[\phi(1,t) - w_x(1,t)] + w_t(0,t)[\phi(0,t) - w_x(0,t)]$$

$$+ \int_0^1 w_t(x,t)[\phi_x(x,t) - w_{xx}(x,t)]\,dx + mW_t(t)W_{tt}(t).$$

Applying BC of Eq. (3.33) - (3.34) and (3.36) - (3.37), the first and the last integral cancel each other (with the last integral rearranged) and the second and the third integrals are combined and then vanished according to (3.42), the equation becomes

$$\dot{V}(t) = \int_0^1 w_t(x,t)[w_{xx}(x,t) - \phi_x(x,t)]\,dx \tag{3.49}$$

$$+ W_t(t)[w_x(1,t) - \phi(1,t)] - \int_0^1 \phi_{xx}(x,t)\phi_t(x,t)\,dx$$

$$+ \int_0^1 \phi_t(x,t) \, [\, \phi(x,t) - w_x(x,t) \,] \, dx \; + \; \int_0^1 w_t(x,t) \, [\, \phi_x(x,t) - w_{xx}(x,t) \,] \, dx$$

$$+ \; m W_t(t) W_{tt}(t).$$

Then, Eq. (3.49) simplifies to

$$\dot{V}(t) \;=\; W_t(t) \, [\, w_x(1,t) - \phi(1,t) \,] \; + \; m \, W_t(t) \, W_{tt}(t). \qquad (3.50)$$

By putting the boundary condition (3.35) into (3.50), yielding

$$\dot{V}(t) \;=\; W_t(t) \, [\, -m \, W_{tt}(t) + U(t) \,] \; + \; m \, W_t(t) \, W_{tt}(t), \qquad (3.51)$$

$$=\; W_t(t) \, [\, -m W_{tt}(t) - c_1 W_t(t) + v(t) \,] \; + \; m \, W_t(t) W_{tt}(t),$$

$$=\; W_t(t) \, [\, -c_1 W_t(t) + v(t) \,].$$

For the sake of stability proving, we let $y = W_t(t)$ be an output of the system and we will obtain

$$\dot{V}(t) \;=\; v(t) \, y(t) \; - \; c_1 \, y^2(t). \qquad (3.52)$$

From Eq. (3.52) and lamma 1, the system Eq. (3.41) – (3.42) with boundary conditions (3.33) - (3.37) and the controller (3.43) is L_2-stable.

Now, the additional control input $v(t)$ will be chosen. Again, the variable $\bar{y} = w(1,t)$ is defined as an output. According to the feedback control theory, we can stabilize the system by the control input $v(t) = -\varphi(\bar{y})$ where φ is a function by which $\varphi(0) = 0$ and $\bar{y}^T \varphi(0) > 0$ for all $\bar{y} \neq 0$, then we choose the control component as shown below,

$$v(t) \;=\; -c_0 \, W(t), \quad k > 0. \qquad (3.53)$$

On the right-hand side of Eq. (3.53) is a spring or elastic force term. Substituting the input (3.53) into the controller (3.43)

$$U(t) \ = \ -c_1 W_t(t) - c_0 W(t). \tag{3.54}$$

Note that the first term on the right-side of Eq. (3.54) is damping force and the second term is spring or elastic force. Due to the fact that the right end of the beam was secured to the base, so $W(t) = w(1,t)$, the controller becomes

$$U(t) \ = \ -c_1 w_t(1,t) - c_0 w(1,t). \tag{3.55}$$

In the controller (3.55), the state feedback variables - both the displacement of the moving base and its time derivative - are employed in the controller of the control scheme. In this instance, the state estimator is unnecessary since we place the sensing and actuation in the same location. In this design, the sensing and actuation setup is called collocated configulation.

The controller's components or terms are relevant to physical variables in a real-world situation. The first term on the right-hand side of (3.55) acts as a damping component used to reduce the vibration. The second term represents the potential energy with a unique minimum at $x = 0$.

The controller obviously uses a proportional-derivative (PD) algorithm. The controller is implemented on the moving base, and the control action is determined by the movements of the base.

3.4 Backstepping Observer Design

In this section, the observer design is presented. This design methodology was proposed by M. Krstic et al. (M. Krstic, B. Z. Guo, A. Balogh, & A. Smyshlyaev, 2008b, pp. 553-574). It is the typical form of the so-called copy of the system plus an injection of the estimation error of the output, which imitates the finite-dimensional case, which will

be explained later. The determination of the observer gains is similar to the one that is used by the Lünberger observer method. For the design technique, the observer error system is changed into a target system that is known to be exponentially stable by using an invertible coordinate transformation. The measurements used in the observer system are measured only at the tip of the beam.

Eq (3.42) can be expressed in the following form

$$\phi_{xx}(x,t) - b^2\phi(x,t) + b^2 w_x(x,t) = 0, \tag{3.56}$$

where $b^2 = 1/\varepsilon$.

Take Laplace transform in x of (3.56), we get,

$$\phi(x) = \cosh(bx)\phi(0) - b\int_0^x \sinh(b(x-y))\, w_y(y)\, dy. \tag{3.57}$$

Integrating by parts the integral term of the right-hand side of the above equation, yields (Krstic, Balogh, et al., 2006a, pp. 1389-1394),

$$\phi(x) = \cosh(bx)\phi(0) + b\sinh(bx)w(0) \tag{3.58}$$

$$- b^2 \int_0^x \cosh(b(x-y))\, w(y)\, dy.$$

By setting $x = 1$ in Eq. (3.58), we can write an expression for $\phi = (0,t)$ given in term of $\phi = (1,t)$ as following,

$$\phi(0) = \frac{1}{\cosh(b)}[\phi(1) - b\sinh(b)w(0) - b^2\int_0^1 \cosh(b(1-y))\, w(y)\, dy]. \tag{3.59}$$

We obtain Eq. (3.60) by substituting it into Eq. (3.58).

$$\phi(x) = \frac{\cosh(bx)}{\cosh(b)} [\phi(1) - b\sinh(b) w(0) - b^2 \int_0^1 \cosh(b(1-y)) w(y) dy] \quad (3.60)$$

$$+ b\sinh(bx) w(0) - b^2 \int_0^x \cosh(b(x-y)) w(y) dy].$$

Differentiating Eq. (3.60) with respect to space, x and substitute into Eq. (3.31), then we get another form of the beam used for the observer model,

$$\varepsilon w_{tt}(x,t) = w_{xx}(x,t) + b^2 w(x,t) + b^3 \int_0^x \sinh(b(x-y)) w(y) dy \quad (3.61)$$

$$- b^2 \cosh(bx) w(0,t) - b\sinh(bx) \phi(0),$$

$$w_x(0) = \phi(0). \quad (3.62)$$

From eq. (3.61) and boundary condition (3.62), the following PDE provides the observer,

$$\varepsilon \hat{w}_{tt}(x,t) = \hat{w}_{xx}(x,t) + b^2 \hat{w}(x,t) + b^3 \int_0^x \sinh(b(x-y)) \hat{w}(y) dy \quad (3.63)$$

$$- b^2 \cosh(bx) w(0,t) + b\sinh(bx) \phi(0,t)$$

$$+ p_y(x,0) (w(0,t) - \hat{w}(0,t),$$

$$\hat{w}_x(0,t) = \phi(0,t) + p(0,0)(w(0,t) - \hat{w}(0,t)) - c_2(w_t(0,t) - \hat{w}_t(0,t)), \quad (3.64)$$

$$\hat{w}(1,t) = w(1,t). \quad (3.65)$$

where $p(x,y)$ is the observer error transformation gain which is to be determined. The design parameter for the observer, c_2 is used in determining the observer's convergence rate.

The observer uses the information of the displacement, $w(0,t)$ and the rotating angle, $\phi(0,t)$, which are both measured at the tip of the beam.

The observer (3.63) – (3.65) is the typical form of the so-called copy of the system plus an injection of the estimation error of the output, which imitates the finite-dimensional case, where the observer of the form $\dot{\hat{x}} = A\hat{x} + Bv + L(y - C\hat{x})$ is used for the state equation $\dot{x} = Ax + Bv$, and the output equation $y = Cx$, where x is the state, y is the output, and v is the input. Notice that the variables x and y will also be used as spatial variables in the controller and observer designs. A, B and C are the system, control, output matrices, respectively, and L the observer gain matrix (Krstic & Smyshlyaev, 2008, pp. 53-54). It should note that the above observer can be used whether the input, $w(1)$ in (3.65) is replaced by other control schemes such as the time-dependent controller or even set to zero.

The approach that is used to determine the gains is similar to the one that is us ed by the Lünberger observer method, which is based on the pole placement concept.

The observer error is introduced,

$$\tilde{w}(x,t) = w(x,t) - \hat{w}(x,t). \tag{3.66}$$

The observer's error dynamics are, therefore,

$$\varepsilon \tilde{w}_{tt}(x,t) = \tilde{w}_{xx}(x,t) + b^2 \tilde{w}(x,t) + b^3 \int_0^x \sinh(b(x-y)) \tilde{w}(y)\, dy \tag{3.67}$$

$$-p_y(x,0)\ \tilde{w}(0,t),$$

$$\tilde{w}_x(0,t) = -p(0,0)\tilde{w}(0,t) + c_2\tilde{w}_t(0,t), \tag{3.68}$$

$$\tilde{w}(1,t) = 0. \tag{3.69}$$

By using the following transformation integral (Krstic et al., 2008b, pp. 553-574),

$$\tilde{w}(x) = \tilde{\upsilon}(x) - \int_0^x p(x,y)\tilde{\upsilon}(y)\, dy. \tag{3.70}$$

to convert the observer error dynamics (3.67) - (3.69) into the following target system

$$\varepsilon \tilde{\upsilon}_{tt}(x,t) = \tilde{\upsilon}_{xx}(x,t), \tag{3.71}$$

$$\tilde{\upsilon}_{x}(0,t) = \tilde{c}_{0}\tilde{\upsilon}_{t}(0,t), \tag{3.72}$$

$$\tilde{\upsilon}(1,t) = 0, \tag{3.73}$$

which has been shown to have exponential stability.

From the transformation of variables, the observer gain will satisfy the following PDE,

$$p_{yy}(x,y) = p_{xx}(x,y) + b^{2}p(x,y) - b^{3}\sinh(b(x-y)),$$

$$+ b^{3}\int_{y}^{x}p(\xi,y)\sinh(b(x-\xi))d\xi, \tag{3.74}$$

$$p(x,x) = \frac{b^{2}}{2}(x-1), \tag{3.75}$$

$$p(1,y) = 0. \tag{3.76}$$

where ξ is the integration variable. This PDE is of hyperbolic type and its domain is a lower triangle and is shown in Figure 15.
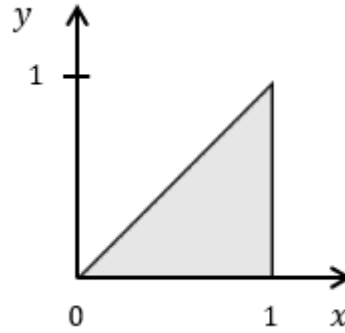
FIGURE 15 The observer-gain kernel's domain.

By solving the above PDE, the observer gains $p(0,0)$ and its derivative $p_y(x,0)$ in (3.63) - (3.65) are obtained. The observer utilizes only the slope and the displacement at the free end of the beam to estimate all values of the displacements in the beam domain and is employed in the design of controllers.

The following lemma establishes the backstepping observer's convergence.

<u>Lemma 3</u> Suppose the classical solution of (3.67) – (3.69) exists. Then the invertible transformation (3.70) converts the error system (3.67)–(3.69) into the already known exponentially stable system (3.71) – (3.73) (Krstic et al., 2008b, pp. 553-574).

Proof

The transformation (3.70), differentiated with respect to x and t, is as follows:

$$\varepsilon \tilde{w}_{tt}(x,t) = \varepsilon \tilde{\upsilon}_{tt}(x,t) - \int_0^x p(x,y)\,\varepsilon \tilde{\upsilon}_{tt}(y,t)\,dy - \tilde{w}_{xx}(x,t) + \tilde{w}_{xx}(x,t), \qquad (3.77)$$

$$= \varepsilon \tilde{\upsilon}_{tt}(x,t) - \int_0^x p_{yy}(x,y)\,\tilde{\upsilon}(y,t)\,dy - p(x,x)\tilde{\upsilon}_x(x,t) + p(x,0)\tilde{\upsilon}_x(x,t)$$

$$+ \; p_y(x,x)\tilde{\upsilon}(x,t) - p_y(x,0)\tilde{\upsilon}(0,t) - \tilde{\upsilon}_{xx}(x,t) + [2p_x(x,x) + p_y(x,x)]\tilde{\upsilon}(x,t)$$

$$+ p(x,x)\tilde{\upsilon}_x(x,t) + \int_0^x p_{xx}(x,y)\,\tilde{\upsilon}(y,t)\,dy + \tilde{w}_{xx}(x,t),$$

$$= \tilde{w}_{xx}(x,t) \; + b^2 \tilde{\upsilon}(x,t) \; + c_2\,p(x,0)\,\tilde{w}_t(0,t) - p_y(x,0)\,\tilde{\upsilon}(0,t)$$

$$+ \int_0^x [\, p_{xx}(x, y) - p_{yy}(x, y) + b^2 p(x, y)\tilde{\upsilon}(y,t)\,]\, dy.$$

Using the observer gain PDE (3.74) – (3.76) in (3.77), we obtain the governing equation (3.71) – (3.73).

Taking the derivative with respect to x of the transformation (3.70) with respect to x and setting $x = 0$:

$$\tilde{w}_x(0,t) \; = \; \tilde{\upsilon}_x(0,t) - p(0,0)\, \tilde{\upsilon}(0,t). \tag{3.78}$$

When comparing (3.78) to the boundary condition (3.68), yielding the following,

$$\tilde{w}_x(0,t) \; = \; - p(0,0)\, \tilde{\upsilon}(0,t) + c_2\, \tilde{\upsilon}_t(0,t). \tag{3.79}$$

So, one obtain the boundary condition of (3.72). Then, the boundary condition of (3.73) is satisfied due to $p(1, y) = 0$. So, the lemma is proved.

Figure 16 shows the diagram of the control with the observer. The sensor located at the beam tip measures the beam's dynamics, $w(0,t)$ and sends the information to the observer for state estimation, $\hat{w}(0,t)$. The estimated state is then fed into the controller and creates the actuator's signal $\hat{w}(0,t)$.
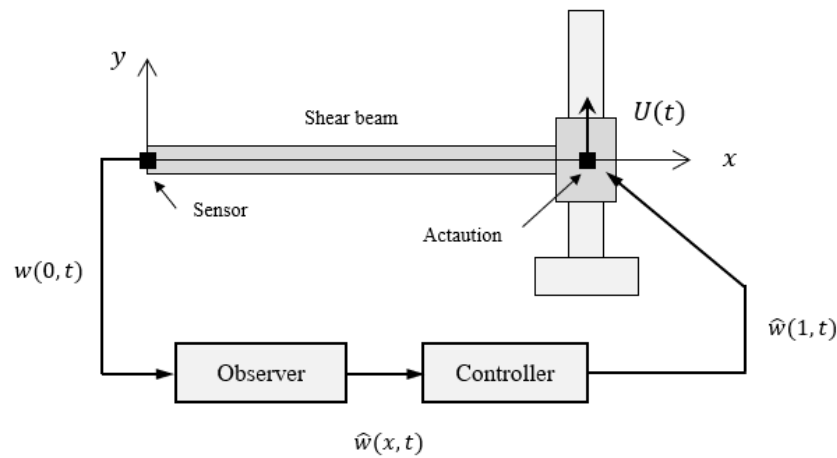
FIGURE 16 The control diagram.

3.5 Chapter conclusion

The technique for designing the passivity-based controller was discussed. To begin, a mathematical model for the shear was constructed using Newton's second law, which also applied to other engineering beams. It was the partial differential equation that represented the shear beam model (PDE). One end of the cantilever shear beam was connected to the moving base, while the other end was free to move. In order to construct a controller, we first defined the passivity of the system and proved that the feedback control is the finite gain L_2- stability. In the passivity-based design, the storage function, which in this study is the energy function, was defined. This function is a representation of both the kinetic energy and the potential energy of the system. The resulting controller was characterized by its elastic and damping components and has a proportional and derivative (PD) control structure. The moving base housed both the sensing and acting components of the control setup. The sensing is at one end and the actuation is at the other in the real-world application or implementation because the control set-up is non-collocated. An observer or the state estimator is required here. The backstepping observer was used in this study. The gain kernel for the observer was developed and implemented. The domain of the hyperbolic PDE gain kernel is a lower triangle. In addition, the observer's convergence was shown.

CHAPTER 4

RESULT

This chapter will present the shear beam system's vibration suppression by the proposed passivity-based controller. The numerical simulation will be performed using the finite difference equations. The results of the controller's performance will be discussed. In Section 4.1, the finite-difference equations used to solve partial differential equations are discussed. In Section 4.2, the finite-difference versions of the partial differential equations for the full-state plant, the observer, and the observer's gain kernel are presented. The simulation and discussion are described in detail in Section 4.3. In Section 4.4, the effects of the different parameter values are shown. The last section of the chapter is the conclusion.

4.1 Finite Difference Equations

In this thesis, the finite difference method (FEM), a form of numerical solution method, is used to solve PDEs. The finite difference approach provides discrete numerical values at a specified grid point (x,t) or (x, y). The numerical values are approximations of continuous solutions.

For shear beam equation, it is assumed that the region to be examnined is covered by uniform rectangular grid with sides paralell to $x-$ and $t-$axis, with Δx and Δt being grid spacing in the $x-$ and $t-$directions, respectively.

For PDE of both shear beam equation and observer, the grid is also uniform rectangular grid with sides paralell to $x-$ and $t-$axis, with Δx and Δy being grid spacing in the $x-$ and $t-$directions, respectively.

Furthermore, the point considered is the point $x_i = i\,\Delta x,\ y_i = i\,\Delta y$, and $t_j = j\,\Delta t$ of the domain, where i and j are integers, where $i = j = 1$ is the origin points and I and J are the maximum integers. The value of function $w(x,t)$ and $p(x,t)$ are denoted by w_i^j and p_i^j, respectively.

In this thesis, the first- and second-order terms in the PDE are solved by using the following finite difference approximations (Mathews & Fink, 2004, pp. 352-504):

The forward finite difference in time,

$$\left(\frac{\partial w}{\partial t}\right)_i^j = \frac{w_i^{j+1} - w_i^j}{\Delta t} + O(\Delta t). \tag{4.1}$$

The backward finite difference in time,

$$\left(\frac{\partial w}{\partial t}\right)_i^j = \frac{w_i^j - w_i^{j-1}}{\Delta t} + O(\Delta t). \tag{4.2}$$

The forward finite difference in space,

$$\left(\frac{\partial w}{\partial x}\right)_i^j = \frac{w_{i+1}^j - w_i^j}{\Delta x} + O(\Delta x). \tag{4.3}$$

The backward finite difference in space,

$$\left(\frac{\partial w}{\partial x}\right)_i^j = \frac{w_i^j - w_{i-1}^j}{\Delta x} + O(\Delta x). \tag{4.4}$$

The centered finite difference in time,

$$\left(\frac{\partial^2 w}{\partial t^2}\right)_i^j = \frac{w_i^{j+1} - 2w_i^j + w_i^{j-1}}{(\Delta t)^2} + O(\Delta t^2). \tag{4.5}$$

The centered finite difference in space,

$$\left(\frac{\partial^2 w}{\partial x^2}\right)_i^j = \frac{w_{i+1}^j - 2w_i^j + w_{i-1}^j}{(\Delta x)^2} + O(\Delta x^2), \tag{4.6}$$

where the terms $O(*)$ is the truncation errors.

Since there are integration terms in the governing equations of the system, so numerical integration is needed. In this thesis, we use a trapezoidal integration rule to solve the definite integral as follows,

$$\int_a^b f(x,t)\, dx \;=\; \frac{\Delta x}{2} f_a \;+\; \sum_{k=a+1}^{b-1} f_k \;+\; \frac{\Delta x}{2} f_b. \tag{4.7}$$

.where $f(x)$ is the function to be integrated, a and b are the limite of integration.

4.2 Numerical Calculations

For the numerical simulation of the shear beam model, the partial derivative terms in the previous section will be solved using the finite difference method (FDM). The forward-backward difference equation in the first order and the centered difference equation in the second order are employed to discretize the first- and second-order variables of the PDEs. Then, we can calculate the integral term by using the trapezoidal integration method.

4.2.1 The finite difference equations for the full-state plant

Using the beam model (3.61), the finite difference equation of the full-state plant is formulated. Figure 17 shows the calculation grid that will be used to do the computations, where Δx and Δy are spatial and temporal increments, i and j are the indices, respectively.
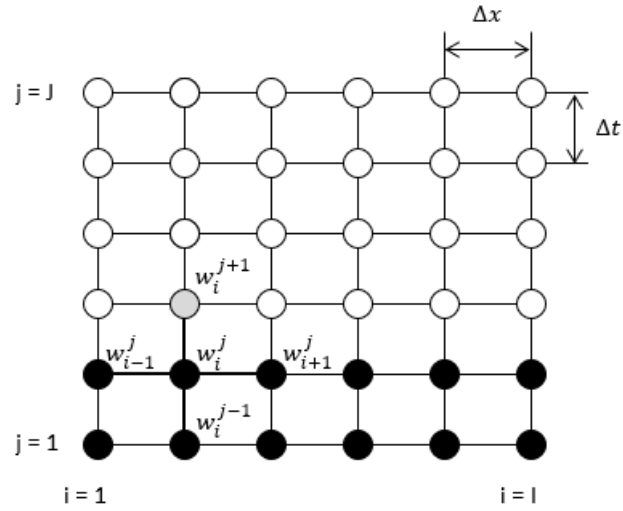
FIGURE 17 The calculation grid for the beam.

Equation (3.61) can be approximated by using the following finite element equation,

$$\varepsilon \frac{w_i^{j+1} - 2w_i^j + w_i^{j-1}}{(\Delta t)^2} = \frac{w_{i+1}^j - 2w_i^j + w_{i-1}^j}{(\Delta x)^2} + b^2 w_i^j \qquad (4.8)$$

$$+ b^3 \, \Delta y \left(\begin{array}{l} \dfrac{1}{2} \sinh[b(x_i - y_1)] \, w_1^j \\[2mm] + \displaystyle\sum_{k=2}^{i-1} \sinh[b(x_i - y_k)] \, w_k^j \\[2mm] + \dfrac{1}{2} \sinh[b(x_i - y_i)] \, w_i^j \end{array} \right) - b^2 \cosh(bx_i) \, w_1^j - b \sinh(bx_i) \, \phi_1^j .$$

Then, we solve for the element w_i^{j+1},

$$w_i^{j+1} = 2w_i^j - w_i^{j-1} + q(w_{i+1}^j - 2w_i^j + w_{i-1}^j) + s b^2 w_i^j \qquad (4.9)$$

$$+ \; sb^3 \Delta y \left(\begin{array}{l} \dfrac{1}{2} \sinh[b(x_i - y_1)] \, w_1^j \\[2mm] +\displaystyle\sum_{k=2}^{i-1} \sinh[b(x_i - y_k)] \, w_k^j \\[2mm] +\dfrac{1}{2}\sinh[b(x_i - y_i)]\, w_i^j \end{array} \right)$$

$$- \; sb^2 \cosh(bx_i)\, w_1^j - \frac{sb}{\Delta x}\sinh(bx_i)(w_2^j - w_1^j).$$

where $r = \Delta t / \Delta x$, $q = r^2 / \varepsilon$ and $s = (\Delta t)^2 / \varepsilon$.

Finally, we obtain the following finite difference equation,

$$w_i^{j+1} \;=\; (2 - 2q - sb^2)\, w_i^j - w_i^{j-1} + q(w_{i+1}^j + w_{i-1}^j) \qquad (4.10)$$

$$+ \; sb^3 \Delta y \left(\begin{array}{l} \dfrac{1}{2} \sinh[b(x_i - y_1)] \, w_1^j \\[2mm] +\displaystyle\sum_{k=2}^{i-1} \sinh[b(x_i - y_k)] \, w_k^j \\[2mm] +\dfrac{1}{2}\sinh[b(x_i - y_i)]\, w_i^j \end{array} \right)$$

$$- \; sb^2 \cosh(bx_i)\, w_1^j - \frac{sb}{\Delta x}\sinh(bx_i)(w_2^j - w_1^j).$$

The elements in the first and second rows can be computed from the given initial conditions as shown in Figure 17.

The elements w_i^{j+1} in the next row from $i=2$ to $i=I-1$ are determined using information from the two preceding rows.

4.2.2 The finite difference equations of the first element for the full-state plant

Since the finite difference equation (4.10) cannot be used to calculate the first element w_i^{j+1} at $x = 0$, Eq. (3.59) and the boundary condition (3.33) are employed as follows,

$$w_x(0,t) = \phi(0,t) = \frac{1}{\cosh(b)} \, [\phi(1,t) - b\sinh(b)\, w(0,t)$$

(4.11)

$$+ \, b^2 \int_0^1 \cosh(b(1-y))\, w(y)\, dy \,].$$

From the boundary condition (3.36), $\phi = (1,t)$,

$$w_x(0,t) = \frac{1}{\cosh(b)} \, [-b\sinh(b)w(0,t) + b^2 \int_0^1 \cosh(b(1-y))\, w(y)\, dy \,].$$

(4.12)

So, the finite difference equation of Eq. (4.12) can be expressed as,

$$\frac{w_2^{j+1} - w_1^{j+1}}{\Delta x} = \frac{1}{\cosh(b)}$$

$$\times \left\{ -b\sinh(b) w_1^{j+1} + b^2 \Delta y \left(\begin{array}{l} \dfrac{1}{2}\cosh[b(1-y_1)]\, w_1^{j+1} \\[2mm] + \displaystyle\sum_{k=2}^{M-1} \cosh[b(1-y_k)]\, w_k^{j+1} \\[2mm] + \dfrac{1}{2}\cosh[b(1-y_I)]\, w_I^{j+1} \end{array} \right) \right\}.$$

(4.13)

$$w_2^{j+1} - w_1^{j+1} = \frac{\Delta x}{\cosh(b)}$$

(4.14)

$$\times \left\{ -b\sinh(b)\,w_1^{j+1} + b^2\Delta y \left(\begin{array}{l} \dfrac{1}{2}\cosh[b(1-y_1)]\,w_1^{j+1} \\[2mm] + \displaystyle\sum_{k=2}^{M-1} \cosh[b(1-y_k)]\,w_k^{j+1} \\[2mm] + \dfrac{1}{2}\cosh[b(1-y_I)]\,w_I^{j+1} \end{array} \right) \right\}.$$

$$w_2^{j+1} + \frac{\Delta x}{\cosh(b)}b\sinh(b)\,w_1^{j+1} - \frac{0.5b^2\Delta x\Delta y}{\cosh(b)}\cosh(b(1-y_1))\,w_1^{j+1} - w_1^{j+1} \ = \qquad (4.15)$$

$$w_1^{j+1} = \frac{\dfrac{b^2\Delta x\Delta y}{\cosh(b)}\left(\begin{array}{l} \displaystyle\sum_{k=2}^{I-1}\cosh[b(1-y_k)]\,w_k^{j+1} \\[2mm] + \dfrac{1}{2}\cosh[b(1-y_I)]\,w_I^{j+1} \end{array} \right).}{b\,\Delta x\tanh(b) - \dfrac{0.5b^2\Delta x\Delta y}{\cosh(b)}\cosh[b(1-y_1)] - 1} \qquad (4.16)$$

$$\times \frac{b^2\Delta x\Delta y}{\cosh(b)}\left(\begin{array}{l} \displaystyle\sum_{k=2}^{I-1}\cosh[b(1-y_k)]\,w_k^{j+1} \\[2mm] + \dfrac{1}{2}\cosh[b(1-y_I)]\,w_I^{j+1} \end{array} \right).$$

$$w_1^{j+1} = \frac{b^2\Delta x\Delta y}{\cosh(b)\left(b\,\Delta x\tanh(b) - \dfrac{0.5b^2\Delta x\Delta y}{\cosh(b)}\cosh[b(1-y_1)] - 1 \right)} \qquad (4.17)$$

$$\times \left(\begin{array}{l} \displaystyle\sum_{k=2}^{I-1}\cosh[b(1-y_k)]\,w_k^{j+1} \\[2mm] + \dfrac{1}{2}\cosh[b(1-y_I)]\,w_I^{j+1} \end{array} \right).$$

The Eq. (4.17) is used to calculate the first elements of each row.

4.2.3 The finite difference equations of the last element for the full-state plant

For the last element, w_I^{j+1} can be computed from the boundary condition (3.35) with the controller, $U(t)$,

$$m \, w_{tt}(1,t) + [\, w_x(1,t) - \phi(1,t) \,] = U(t) \tag{4.18}$$

$$m \, w_{tt}(1,t) + [\, w_x(1,t) - \phi(1,t) \,] = -c_1 w_t(1,t) - c_0 w(1,t). \tag{4.19}$$

Because of the boundary condition (3.36), $\phi(1,t) = 0$ so

$$m \, w_{tt}(1,t) + w_x(1,t) = -c_1 w_t(1,t) - c_0 w(1,t) \tag{4.20}$$

$$w_x(1,t) = -m \, w_{tt}(1,t) - c_1 w_t(1,t) - c_0 w(1,t). \tag{4.21}$$

The finite difference equation of Eq. (4.21) is written as follows,

$$\frac{w_I^j - w_{I-1}^j}{\Delta x} = -m \, \frac{w_I^{j+1} - 2w_I^j + w_I^{j-1}}{(\Delta t)^2} - c_1 \frac{w_I^j - w_I^{j-1}}{\Delta t} - c_0 \, w_I^j, \tag{4.22}$$

$$m \, \frac{w_I^{j+1} - 2w_I^j + w_I^{j-1}}{(\Delta t)^2} = -\frac{w_I^j - w_{I-1}^j}{\Delta x} - c_1 \frac{w_I^j - w_I^{j-1}}{\Delta t} - c_0 \, w_I^j,$$

$$w_I^{j+1} - 2w_I^j + w_I^{j-1} = -\frac{(\Delta t)^2}{m \Delta x}(w_I^j - w_{I-1}^j) - c_1 \frac{\Delta t}{m}(w_I^j - w_I^{j-1}) - c_0 \frac{(\Delta t)^2}{m} w_I^j,$$

$$w_I^{j+1} = \left(2 - \frac{(\Delta t)^2}{m \Delta x} - c_1 \frac{\Delta t}{m} - c_0 \frac{(\Delta t)^2}{m}\right) w_I^j + \left(c_1 \frac{\Delta t}{m} - 1\right) w_I^{j-1} + \frac{(\Delta t)^2}{m \Delta x} w_{I-1}^j. \tag{4.23}$$

Eq. (4.23) is used to calculate the last element w_I^{j+1} of each row. Note that the displacement of this point is also the displacement of the moving base.

In summary, Eq. (4.10), (4.17) and (4.23) are used to calculate the elements of the full-state plant.

4.2.4 The finite difference equations for the observer

In this subsection, the observer will be developed into the finite difference equation. The finite difference equation for the boundary condition (3.62), at $i = 1$, may be expressed as follows:

$$\frac{\hat{w}_{i+1}^{j} - \hat{w}_{i}^{j}}{\Delta x} = \phi_{1}^{j},$$

$$\phi_{1}^{j} = \frac{\hat{w}_{2}^{j+1} - \hat{w}_{1}^{j}}{\Delta x}. \tag{4.23}$$

From Eq. (3.63), the finite difference equation of the observer be written as follows,

$$\varepsilon \frac{\hat{w}_{i}^{j+1} - 2\hat{w}_{i}^{j} + \hat{w}_{i}^{j-1}}{(\Delta t)^{2}} = \frac{\hat{w}_{i+1}^{j} - 2\hat{w}_{i}^{j} + \hat{w}_{i-1}^{j}}{(\Delta x)^{2}} + b^{2}\hat{w}_{i}^{j} \tag{4.24}$$

$$+ b^{3}\Delta y \left(\begin{array}{c} \dfrac{1}{2}\sinh[b(x_{i} - y_{1})]\,\hat{w}_{1}^{j+1} \\[2mm] +\displaystyle\sum_{k=2}^{i-1} \sinh[b(x_{i} - y_{k})]\,\hat{w}_{k}^{j+1} \\[2mm] +\dfrac{1}{2}\sinh[b(x_{i} - y_{i})]\,\hat{w}_{i}^{j+1} \end{array} \right) - b^{2}\cosh(bx_{i})\,\hat{w}_{1}^{j}$$

$$- b\sinh(bx_{i})\phi_{1}^{j} + (p_{y})_{i}^{1}(w_{1}^{j} - \hat{w}_{1}^{j}),$$

$$\hat{w}_{i}^{j+1} = 2\hat{w}_{i}^{j} - \hat{w}_{i}^{j-1} + q(\hat{w}_{i+1}^{j} - 2\hat{w}_{i}^{j} + \hat{w}_{i}^{j+1}) + sb^{2}\hat{w}_{i}^{j} \tag{4.25}$$

$$+ sb^3\Delta y \left(\begin{array}{l} \dfrac{1}{2} \sinh\left[b(x_i - y_1)\right] \hat{w}_1^j \\[2mm] + \displaystyle\sum_{k=2}^{i-1} \sinh\left[b(x_i - y_k)\right] \hat{w}_k^j \\[2mm] + \dfrac{1}{2} \sinh\left[b(x_i - y_i)\right] \hat{w}_i^j \end{array} \right) - sb^2 \cosh(bx_i)\hat{w}_1^j$$

$$- sb \sinh(bx_i) \left(\frac{\hat{w}_2^j - \hat{w}_1^j}{\Delta x} \right) - s(p_y)_i^1 (w_1^j - \hat{w}_1^j).$$

where $r = \Delta t/\Delta x$, $q = r^2/\varepsilon$ and $s = (\Delta t)^2/\varepsilon$.

$$\hat{w}_i^{j+1} = (2 - 2q + sb^2)\,\hat{w}_i^j - \hat{w}_i^{j-1} + q(\hat{w}_{i+1}^j + \hat{w}_{i-1}^j) \tag{4.26}$$

$$+ sb^3\Delta y \left(\begin{array}{l} \dfrac{1}{2} \sinh\left[b(x_i - y_1)\right] \hat{w}_1^j \\[2mm] + \displaystyle\sum_{k=2}^{i-1} \sinh\left[b(x_i - y_k)\right] \hat{w}_k^j \\[2mm] + \dfrac{1}{2} \sinh\left[b(x_i - y_i)\right] \hat{w}_i^j \end{array} \right) - sb^2 \cosh(bx_i)\hat{w}_1^j$$

$$- \frac{sb}{\Delta x} \sinh(bx_i) \left(\hat{w}_2^j - \hat{w}_1^j \right) + s(p_y)_i^1 (w_1^j - \hat{w}_1^j).$$

Eq. (4.26) is used to calculate the elements of the observer from $i = 2$ to $i = I - 1$.

4.2.5 The finite difference equations of the first and last elements for the observer

Since the first element of each row cannot be determined using Eq. (4.26), so, the finite difference equation will be developed for this element

From the boundary condition (3.64), the finite difference equation can be written as follows,

$$\left(\frac{\hat{w}_{i+1}^{j} - \hat{w}_{i}^{j}}{\Delta x}\right)_{i=1} = \phi_{1}^{j} + p_{1}^{1}(w_{1}^{j} - \hat{w}_{1}^{j}) - c_{2}\left(\frac{w_{1}^{j} - w_{1}^{j-1}}{\Delta t} - \frac{\hat{w}_{1}^{j} - \hat{w}_{1}^{j-1}}{\Delta t}\right), \qquad (4.27)$$

$$\frac{\hat{w}_{2}^{j} - \hat{w}_{1}^{j}}{\Delta x} = \left(\frac{w_{2}^{j} - w_{1}^{j}}{\Delta x}\right) + p_{1}^{1}(w_{1}^{j}) - p_{1}^{1}(\hat{w}_{1}^{j}) - c_{2}\left(\frac{w_{1}^{j} - w_{1}^{j-1}}{\Delta t}\right)$$

$$+ c_{2}\left(\frac{\hat{w}_{1}^{j}}{\Delta t}\right) - c_{2}\left(\frac{\hat{w}_{1}^{j-1}}{\Delta t}\right),$$

$$\hat{w}_{2}^{j} = \hat{w}_{1}^{j} + w_{2}^{j} - w_{1}^{j} + \Delta x\, p_{1}^{1}(w_{1}^{j}) - \Delta x\, p_{1}^{1}(\hat{w}_{1}^{j}) - \frac{c_{2}}{r}(w_{1}^{j} - w_{1}^{j-1}) \qquad (4.28)$$

$$+ \frac{c_{2}}{r}(\hat{w}_{1}^{j}) - \frac{c_{2}}{r}(\hat{w}_{1}^{j-1}),$$

$$\hat{w}_{1}^{j} - \Delta x\, p_{1}^{1}(\hat{w}_{1}^{j}) + \frac{c_{2}}{r}(\hat{w}_{1}^{j}) = \hat{w}_{2}^{j} - w_{2}^{j} + (1 - \Delta x\, p_{1}^{1})\, w_{1}^{j} \qquad (4.29)$$

$$+ \frac{c_{2}}{r}\left(w_{1}^{j} - w_{1}^{j-1} + \hat{w}_{1}^{j-1}\right).$$

We solve for the element $\hat{w}_{1}^{j}$,

$$\hat{w}_{1}^{j} = \frac{1}{1 - \Delta x\, p_{1}^{1} + \dfrac{c_{2}}{r}} \qquad (4.30)$$

$$\times \left\{\hat{w}_{2}^{j} - w_{2}^{j} + (1 - \Delta x\, p_{1}^{1})\, w_{1}^{j} + \frac{c_{2}}{r}\left(w_{1}^{j} - w_{1}^{j-1} + \hat{w}_{1}^{j-1}\right)\right\}.$$

At for the element at $j = j+1$, Eq. (4.30) becomes

$$\hat{w}_{1}^{j+1} = \frac{1}{1 - \Delta x\, p_{1}^{1} + \dfrac{c_{2}}{r}} \qquad (4.31)$$

$$\times \left\{ \hat{w}_2^{j+1} - w_2^{j+1} + (1 - \Delta x \, p_1^1) w_1^{j+1} + \frac{c_2}{r} \left(w_1^{j+1} - w_1^j + \hat{w}_1^j \right) \right\}.$$

The first element of the observer's finite difference equation is given by (4.31), while the final element's finite difference equation is derived from (3.65), as shown below:

$$\hat{w}_I^{j+1} = w_I^{j+1}. \tag{4.32}$$

In summary, Eq. (4.26), (4.31) and (4.32) are used to calculate the elements of the observer.

4.2.6 The finite-difference equations for the observer gain kernel

Lastly, in this subsection, the finite difference equations for the observer gain kernel PDE are formulated. The domain of this PDE is the lower triangle $0 \le y \le x \le 1$, so, Figure 18 depicts the calculating grid with the spatial increments Δx and Δy, and indexed by i and j, respectively.
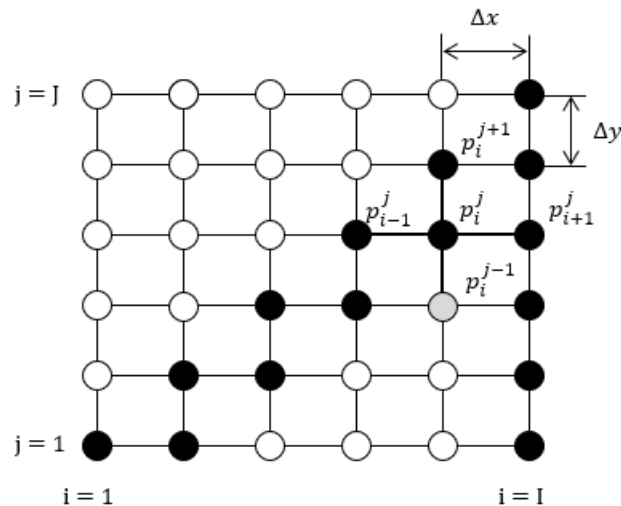
FIGURE 18 Calculation grid for the observer.

From Eq. (3.75), we can get the diagonal elements, p_i^i as follows

$$p_i^i = \frac{b^2}{2}(x_i - 1).$$ (4.33)

Next, to obtain the off-diagonal elements, p_{i+1}^j which are just below the diagonal by differentiating Eq. (3.75) with respect to x, so we obtain,

$$p_x(x, x) = \left(\frac{\partial p(x, y)}{\partial x}\right)_{y=x} = \frac{b^2}{2}.$$ (4.34)

So, the finite difference equation of Eq. (4.34) is as follows,

$$\left(\frac{p_{i+1}^j - p_i^j}{\Delta x}\right)_{j=i} = \frac{b^2}{2}.$$ (4.35)

Then, we get the off-diagonal elements by setting $j = i$ yields

$$p_{i+1}^i = p_i^i + \frac{b^2}{2}\Delta x.$$ (4.36)

The vertical elements at $i = I$ can be obtained by using Eq. (3.76), which are all zero,

$$p_I^j = 0.$$ (4.37)

Now, the rest of the elements are obtained by using Eq. (3.74), so, the observer gain kernel's finite-difference equation is as follows:

$$\frac{p_i^{j+1} - 2p_i^j + p_i^{j-1}}{(\Delta x)^2} = \frac{p_{i+1}^j - 2p_i^j + p_{i-1}^j}{(\Delta x)^2} + b^2 p_i^j - b^3 \sinh(b(x_i - y_j))$$ (4.38)

$$+ b^3 \Delta x \left(\begin{array}{l} \dfrac{1}{2} p_j^j \sinh[b(x_i - y_j)] \\[2ex] + \displaystyle\sum_{k=j+1}^{i-1} p_k^j \sinh[b(x_i - y_k)] \\[2ex] + \dfrac{1}{2} p_i^j \sinh[b(x_i - y_i)] \end{array} \right),$$

$$p_i^{j+1} + p_i^{j-1} = p_{i+1}^j + p_{i-1}^j + (\Delta x)^2 b^2 p_i^j - (\Delta x)^2 b^3 \sinh(b (x_i - y_j)) \qquad (4.39)$$

$$+ (\Delta x)^3 b^3 \left(\begin{array}{l} \dfrac{1}{2} p_j^j \sinh[b(x_i - y_j)] \\[2ex] + \displaystyle\sum_{k=j+1}^{i-1} p_k^j \sinh[b(x_i - y_k)] \\[2ex] + \dfrac{1}{2} p_i^j \sinh[b(x_i - y_i)] \end{array} \right).$$

So, we obtain the finite difference equation for calculating the rest of the elements of the observer gain kernel as follows,

$$p_i^{j-1} = p_{i+1}^j + p_{i-1}^j - p_i^{j+1} + (\Delta x)^2 b^2 p_i^j - (\Delta x)^2 b^3 \sinh(b (x_i - y_j)) \qquad (4.40)$$

$$+ (\Delta x)^3 b^3 \left(\begin{array}{l} \dfrac{1}{2} p_j^j \sinh[b(x_i - y_j)] \\[2ex] + \displaystyle\sum_{k=j+1}^{i-1} p_k^j \sinh[b(x_i - y_k)] \\[2ex] + \dfrac{1}{2} p_i^j \sinh[b(x_i - y_i)] \end{array} \right),$$

$$p_i^{j-1} = p_{i+1}^j + p_{i-1}^j - p_i^{j+1} + (\Delta x)^2 b^2 p_i^j - (\Delta x)^2 b^3 \sinh(b (x_i - y_j)) \qquad (4.41)$$

$$+ (\Delta x)^3 b^3 \left(\begin{array}{l} \dfrac{1}{2} p_j^{\,j} \sinh\left[b(x_i - y_j)\right] \\[4pt] + \displaystyle\sum_{k=j+1}^{i-1} p_k^{\,j} \sinh\left[b(x_i - y_k)\right] \\[4pt] + \dfrac{1}{2} p_i^{\,j} \sinh\left[b(x_i - y_i)\right] \end{array} \right).$$

The equation (4.41) is calculated downward from above, here the known values are available.

Finally, the equation for derivative of the observer gain kernel used in Eq. (3.63) is

$$p_y(x,0) = \left(\frac{p_i^{\,j+1} - p_i^{\,j}}{\Delta y} \right)_{j=1} = \frac{p_i^2 - p_i^1}{\Delta y}. \tag{4.42}$$

In summary, the finite difference equations (4.33), (4.36), (4.37), (4.41) and (4.42) are used to calculate the observer gain kernel PDE.

4.3 Simulation results and Discussions

The beam simulations are shown in this section for both with and without the observer. In solving the partial differential equation, the finite difference equations developed in the preceding section will be implemented.

The numerical computations are performed through the use of code written in MATLAB using the parameters as shown in the Table 1 below. In the numerical simulation, the time and spatial increments are $\Delta t = 0.01$ and $\Delta x = 0.025$, respectively.

TABLE 1 Control parameters

m	ε	c_0	c_1	c_2
0.05	1	1.0	1.25	0.75

The following initial conditions as proposed by Krstic et al. (Krstic, Balogh, & Smyshlyaev, 2006b, pp. 2430-2435) cause the beam to begin vibrating,

$$w(0) = +0.1 (1-x)^2 \cdot \sin [1.6\pi (1-x)], \tag{4.36}$$

$$w_t(0) = -0.1 (1-x)^2 \cdot \sin [1.6\pi (1-x)]. \tag{4.37}$$

Figure 19 illustrates the displacement and velocity at the beginning of the motion as defined by the equations (4.36) and (4.37). The initial conditions are then enhanced by 50% for the observer.
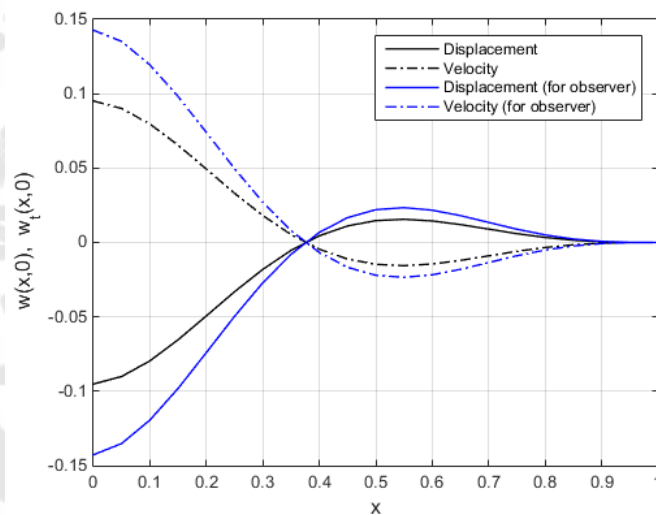

FIGURE 19 Initial displacement and velocity

In the uncontrolled case, the initial conditions are applied to the beam model to stimulate the vibration. The energy of the system is preserved in the beam because there is no damping component in the beam model. Within the system, there are only changes from one form to another between potential and kinetic energy. Figure 20 depicts the oscillating motion of the response. Figure 21 depicts the tip displacement.
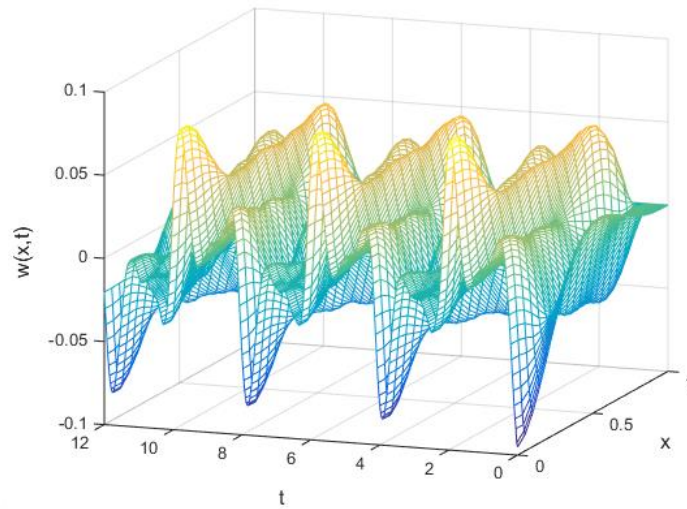
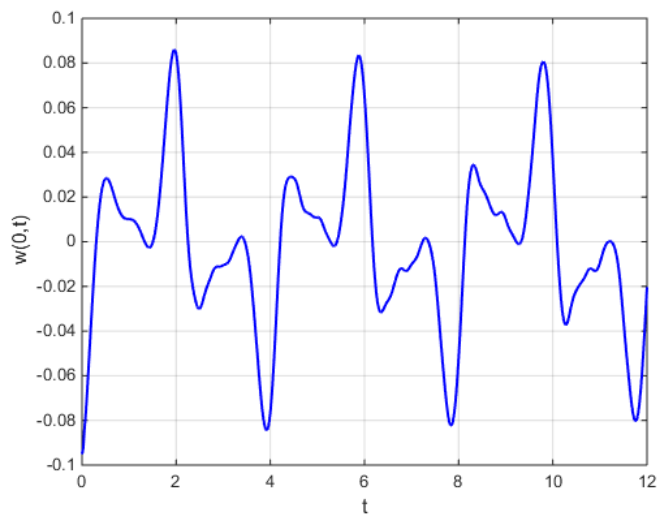FIGURE 20 The simulation for the beam without the controller

FIGURE 21 The displacement of the tip of the beam without the controller.

The beam response in the controlled case, where the controller (22) was applied at the moving base, is shown in Figure 22. The control action and the tip displacements are shown in Figure 23. The vibration quickly died down. This is because the vibrating energy in the system is dissipated through the damping component, $-c_1 w_t(1,t)$ in the controller and the elastic component, $-c_0 w(1,t)$ causing the equilibrium point being at $x = 0$.
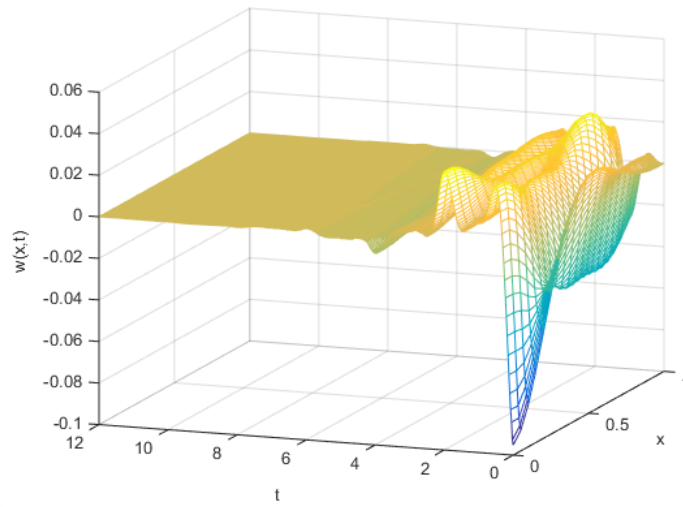
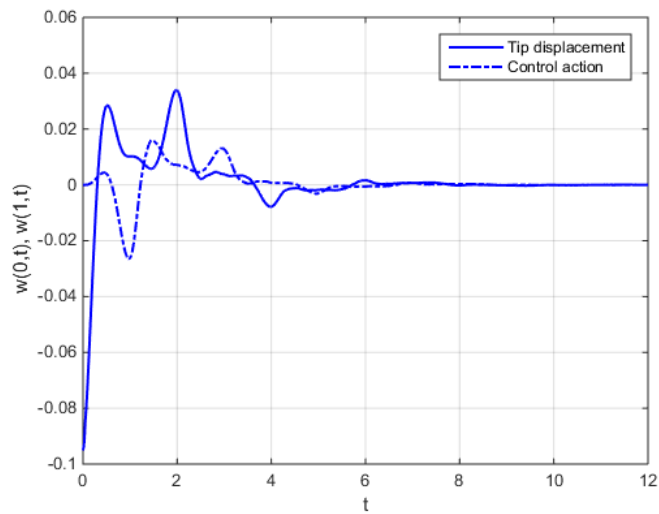FIGURE 22 The simulation for the beam with the controller.

FIGURE 23 The tip displacement and the control action.

Figures 24 and 25 illustrate the observer's gain kernel and its derivative, respectively. The curves were both smooth.
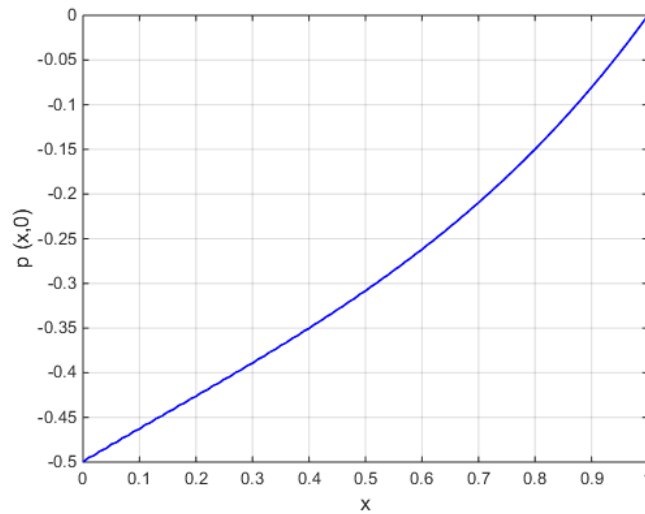
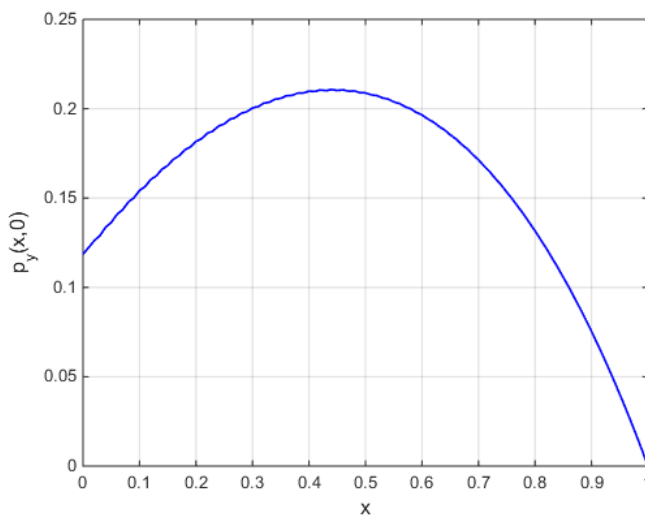FIGURE 24 The observer's gain function.

FIGURE 25 The observer's derivative gain function.

The beam model simulation with observer (3.63) – (3.65) and the controller (3.55) is shown in Figure 26. The observer makes use of the displacement, $w(0,t)$, of the beam's tip and the slope $\phi(0,t)$, which can be derived from the boundary condition (3.33). The initial conditions for the system with the observer, which were 50% larger

than for the full-state system, have caused vibration. In the L_2- sense, the beam is also stabilized.
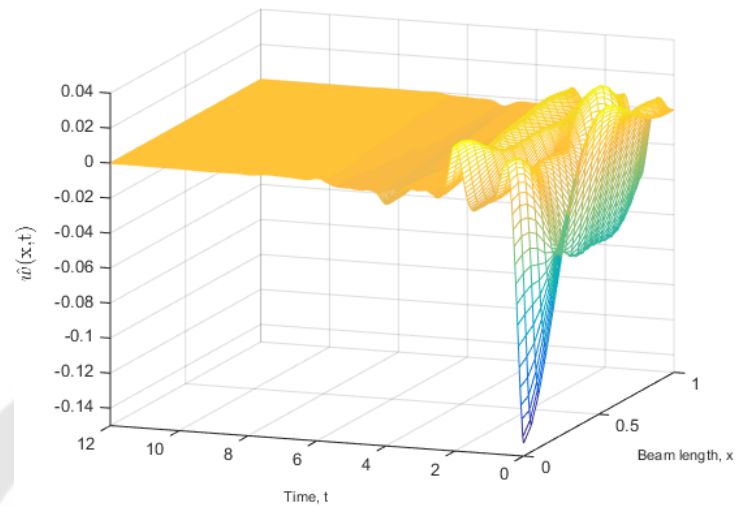

FIGURE 26 The beam simulation with the observer.

Figure 27 depicts the time sequence of the beam displacement snapshots for the uncontrolled case. The solid line represents the full-state response, whereas the dashed line represents the observer's response. Since there is no dampening to reduce the vibration, the beam vibrates indefinitely. Figure 28 shows the snapshots of the beam displacements with the controller at $x = 1$, the responses settle down and reach equilibrium. Notice that the base movements are present at $x = 1$.
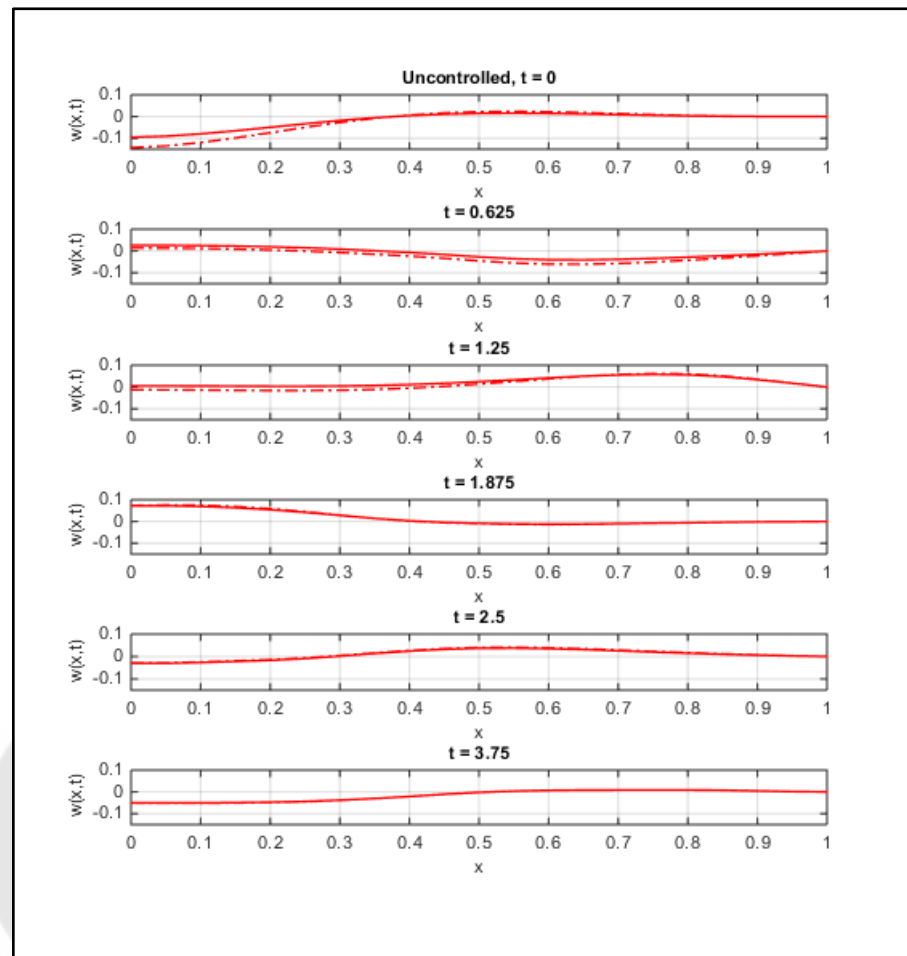
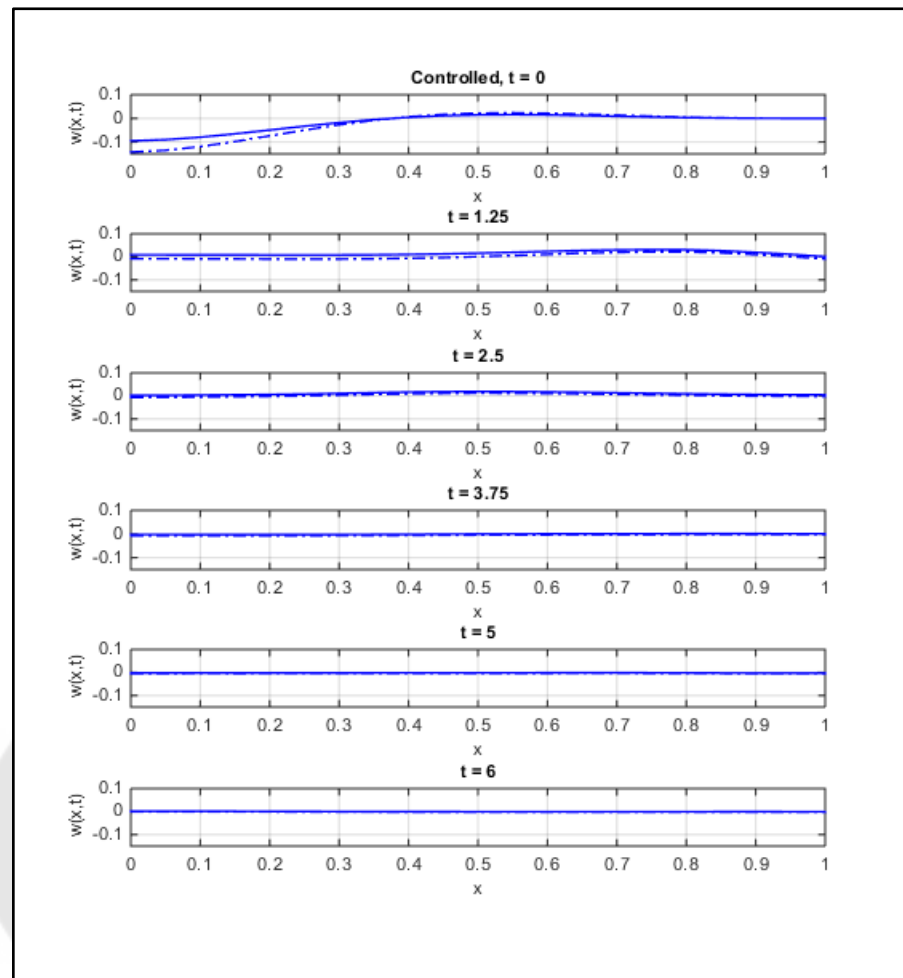FIGURE 27 Snapshots of the uncontrolled beam with the observer.

FIGURE 28 Snapshots of the controlled system with the observer.

Using the L_2- norm, often known as the Euclidean norm, we can calculate the total energy of the system using (4.38) (Khalil, 2002, p. 647).

$$\| w \|_2 = \sqrt{ |w_1|^2 + \cdots + |w_I|^2 } \ . \tag{4.38}$$

The settling time measures how quickly the response settles down. The settling time is defined as the amount of time needed for the beam's norm to reduce to within 2% of its maximum norm under the initial conditions.
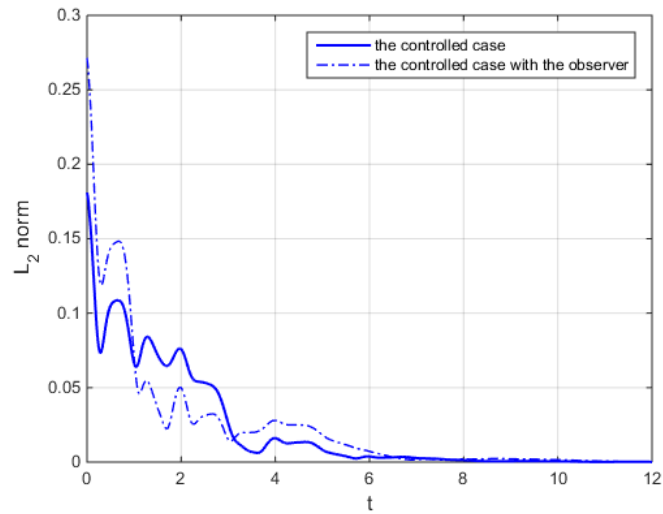
FIGURE 29 The Euclidean norm of the system with and without the observer.

For the full-state plant, the settling time was at $t = 5.9$, whereas in the control with the observer, it was at $t = 5.7$. The time it took the observer to settle down was less than in the full-state case. This depends on the setting of the observer's design parameter, c_2. The system's L_2- norms without and with the observer (solid and dot-dash lines, respectively) are displayed in Figure 29. The energy of the system was quickly dissipated.

The observer error between the full state and the observer is shown in Figure 30. As $t \rightarrow \infty$, the observer error response approaches zero.
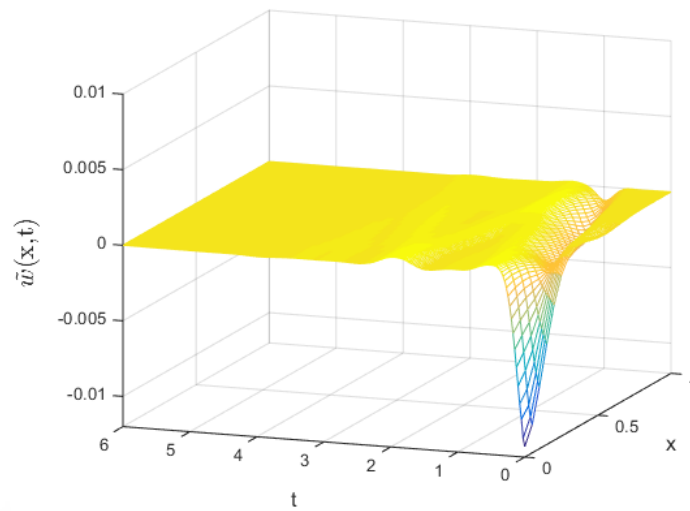
FIGURE 30 The observer error.

4.4 Control and observer with different parameters

The control system's performance will be examined in this section, along with the impact of parameter modifications. Each spring, damping, and observer's design parameter will be changed, but all the other parameters will be kept fixed (Boonkumkrong, Chinvorarat, & Asadamongkon, 2022, pp. 1-11).

4.4.1 The effects of the different spring parameters

In the first case, the damping parameter, c_1 and the observer's design parameter, c_2 will be kept at 1.0 and 0.75, respectively, while the spring parameters, c_0 will be set at 1.0, 1.5, and 2.0. Figures 31 and 32 show the tip displacement of the full-state control and the tip displacement of the control with an observer, respectively.
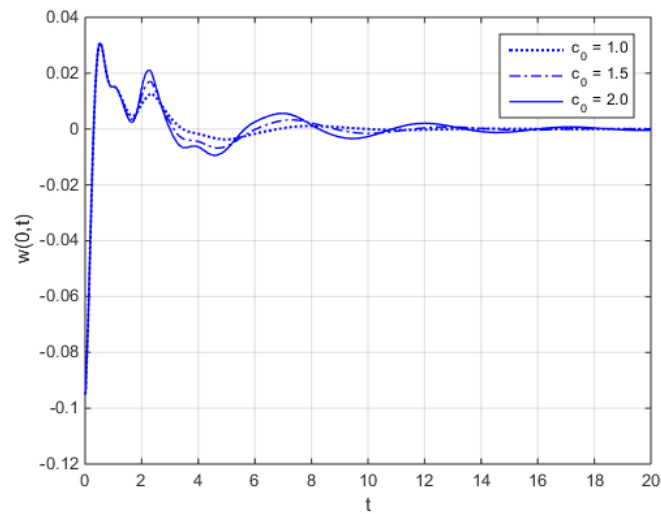
FIGURE 31 The tip displacement with different spring parameters.
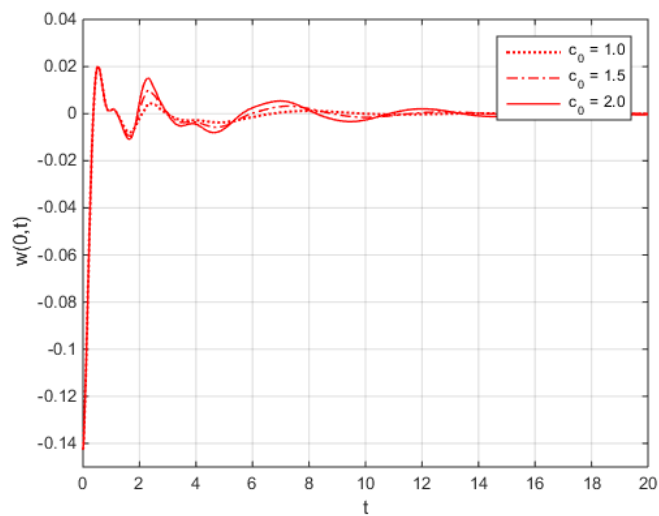
FIGURE 32 The tip displacement *(observer)* with different spring parameters.

The settling times of the different spring parameter, c_0 at the value of 1.0, 1.25, 1.5, 1.75 and 2.0 are displayed in Table 2, and are plotted using the least-squared curve-fitting as shown in Figure 33. As the spring parameter value increased, the settling time also increased. This occurred due to the stiffer spring parameter controller supplying the system with more energy than the softer ones. Notice that the settling

times of the observers were less than that of the full-state case. This was because of the tuning of the design parameter, c_2 for setting the convergence rate of the observer. The spring parameter c_0 is responsible for maintaining the system's equilibrium condition at $w = 0$. The spring parameter should be set at the smallest value possible.

TABLE 2 Settling times for different spring parameters.

Spring	$c_0 = 1.0$	$c_0 = 1.25$	$c_0 = 1.50$	$c_0 = 1.75$	$c_0 = 2.0$
Full-state	5.9	8.0	8.1	10.3	12.3
Observer	5.4	5.5	7.7	7.8	9.9
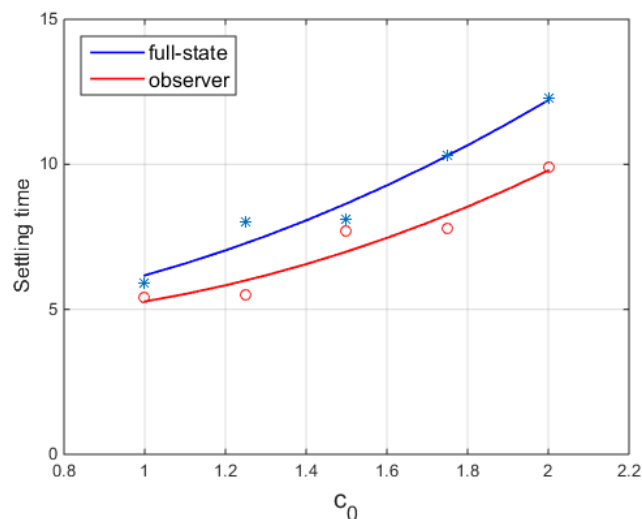
FIGURE 33 Settling times with different spring parameters.

4.4.2 The effects of the different damping parameters

In the second case, the damping parameters, c_1 are varied at the values of 0.5, 0.75, and 1.0, while the spring parameter, c_0 and the observer's design parameter, c_2 are set at 1.0 and 0.75, respectively. Figure 34 for the tip displacement of the full-state control and Figure 35 for tip displacement of the control with an observer. The system where the damping parameter has the smallest value has the largest amplitude.
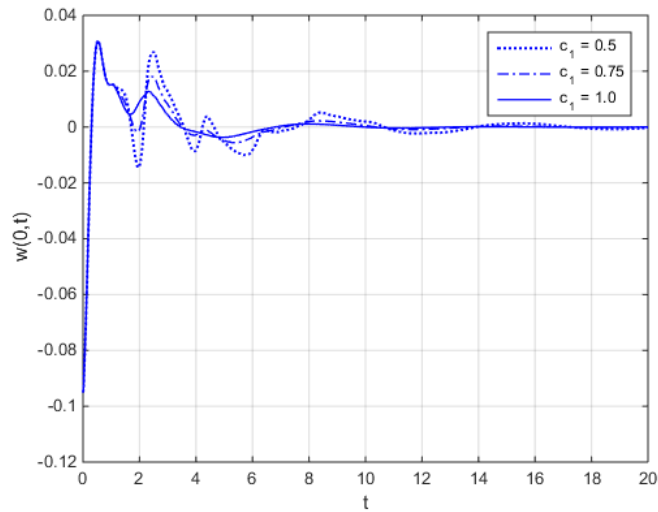
FIGURE 34 Tip displacements with different damping parameters.
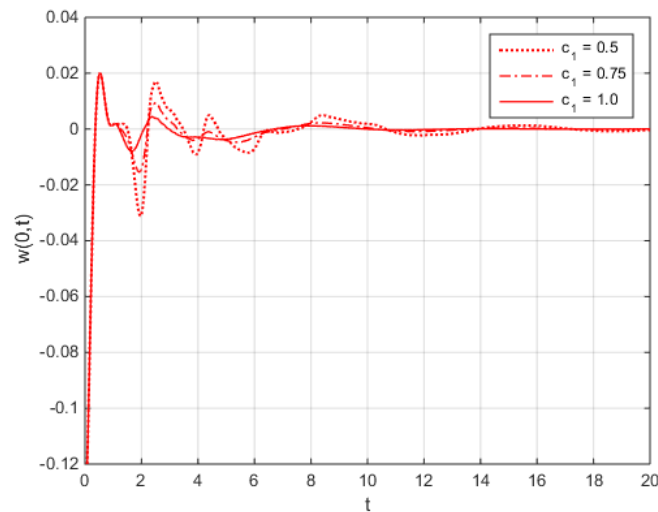
FIGURE 35 Tip displacements (observer) with different damping parameters.

The settling times for the damping parameters, c_1 at various values, including 0.5, 0.75, 1.0, 1.25, and 1.5, are shown in Table 3, and were plotted using the least-squared curve-fitting as shown in Figure 36. The settling time was less in the case of the strong damping parameter. This is because the rate of vibration energy dissipation is high. As we changed the spring parameter up to a certain point, i.e., at

around $c_1 = 1.1$, the time it took for the system to settle started to increase. The reason is that the controller put too much damping into the system, making it move slowly.

TABLE 3 Settling times for different damping parameters.

Damping	$c_1 = 0.5$	$c_1 = 0.75$	$c_1 = 1.0$	$c_1 = 1.25$	$c_1 = 1.5$
Full-state	12.8	8.9	5.9	5.2	4.5
Observer	9.3	6.05	5.4	5.2	4.7
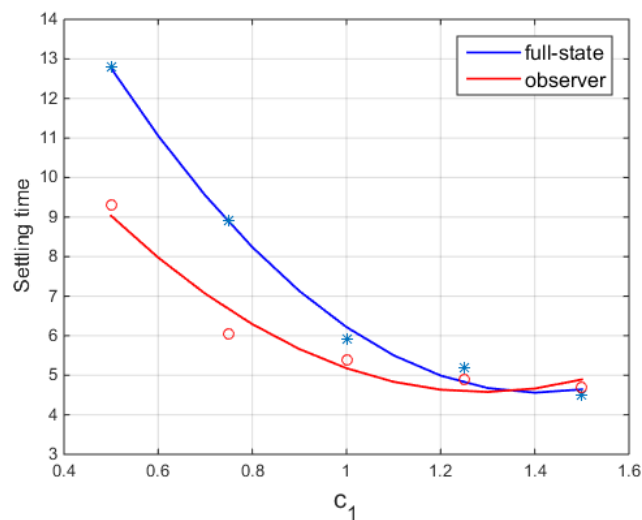
FIGURE 36 Settling times with different damping parameters.

4.4.3 The effects of the different observer's design parameters

For the varying design parameters of the observer, c_2 the control parameters were fixed at $c_0 = 1$, and $c_1 = 1$. The observer's design parameters will be varied at 1.0, 1.5, 2.0, 2.5 and 3.0. The tip displacement of the beam as a result of varying the parameters to 1.0, 2.0, and 3.0 is depicted in Figure 37.
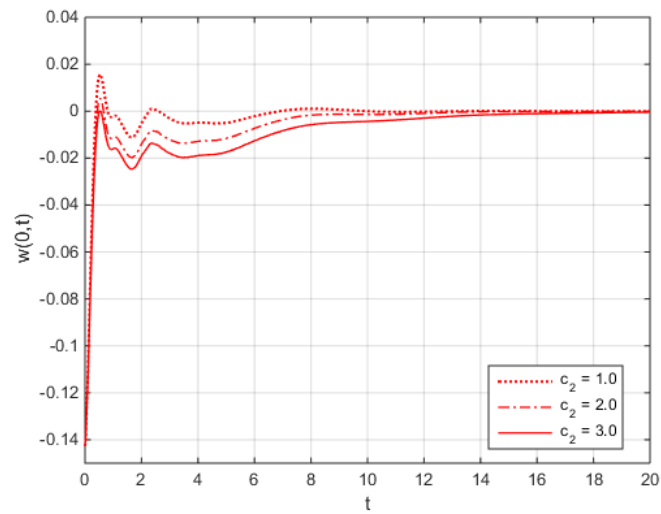
FIGURE 37 Tip displacements with different observer's design parameters.

Table 4 and Figure 38 depict settling times upon varying the observer's design parameters. The settling time increased as the parameter values increased. This parameter is used as a tuning parameter for setting the observer's convergence rate.

TABLE 4 Settling times for the different observer parameters.

Observer	$c_2 = 1.0$	$c_2 = 1.5$	$c_2 = 2.0$	$c_2 = 2.5$	$c_2 = 3.0$
Parameter	5.8	6.5	7.3	9.6	12.2

FIGURE 38 Setting times with different observer's parameters.

4.5 Chapter conclusion

In the first part of the chapter, the finite difference equations to find the solutions of the PDE for the shear beam system, the observer, and the observer gain kernel were developed. The only first- and second-order partial derivative terms and the integr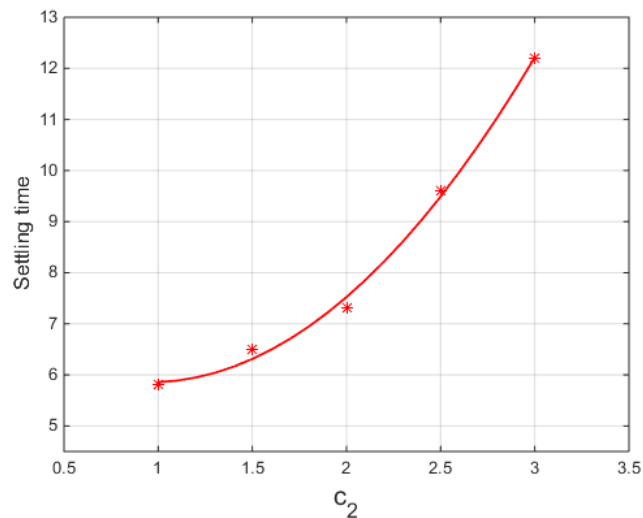ation terms make up the PDE, and the finite difference method makes it easy to solve them. In the second part of the chapter, the numerical simulations were performed. The initial displacement and initial velocity functions were provided. These initial conditions gave the starting information for the subsequent calculations and also triggered the beam systems to vibrate. The numerical simulations were shown in uncontrolled and controlled situations and for both full-state and observer cases. The system responses of both the full-state and observer cases were observed in the controlled case, and they converged satisfactorily to equilibrium at $w = 0$. The energy dissipation due to the damping term in the controller was observed using the Euclidean or $L_2 -$ norm. The error between the responses of the full state and the observer approaches zero as $t \to \infty$. The control parameters, both spring parameter, c_0 and damping parameter, c_1 and the observer's design parameter, c_2 were varied to study the performance of the controller and the observer. The spring, or elastic parameter, in the controller was used to keep

the equilibrium point at $w = 0$, which should be set at a moderate value. The damping parameter is the tuning parameter that determines how long it takes for the control to settle. The higher the value, up to a certain value, the shorter the settling time. If the damping parameter was set too high, the control was slow, or the settling time was longer. For the observer's design parameter, the higher the setting, the longer the settling time. As shown in the simulations, all the parameters were easily tuned. The simulation results have shown that the proposed passivity-based controller effectively eliminated the beam vibration.

CHAPTER 5

SUMMARY DISCUSSION AND SUGGESTION

5.1 Summary Discussion

The boundary control based on passivity has suppressed the flexible beam's vibration. In this study, the undamped shear beam was taken into consideration. By incorporating an energy idea into the design of the controller for this method. The PDE in the beam model may be solved without resorting to a reduced model. The model's higher terms were not excluded; the control spill-over can be avoidable. In the design of the controller, this technique took advantage of the passivity property of the beam. The energy function of the beam was employed as the storage function. It was composed of kinetic and potential energies and was next employed to identify the controller. It was shown that the feedback control system is finite gain L_2 − stable. The damping-spring mechanism dynamics, which were physical variables, were included in the designed controller.

The movable base at the right end of the beam was used for applying the designed controller. Both the actuation and sensing were collocated, which means they were applied in the same place. In the situation of non-collocational architecture, i.e., when the sensing and actuation were located at opposing ends, the backstepping observer was utilized for the estimation of the system's state. The latter configuration can be employed easily in actual applications. With the use of the finite difference method, the PDE was solved numerically. For the numerical calculation, the parameters were set at $\varepsilon = 1, \ m = 0.05, \ c_0 = 1$ and $c_1 = 1.25$ for the controller and $c_2 = 0.75$ for the observer. The time and space increments were $\Delta t = 0.01$ and $\Delta x = 0.025$, respectively. The amount of energy still stored in the system was measured using the Euclidean or L_2 − norm. The beam control simulation results were displayed both with and without the state estimation. The settling time for

the full-state system and the observer were at $t = 5.9$ and $t = 5.7$, respectively. The observer error approached zero as $t \rightarrow \infty$. The proposed control law was simple and successfully removing the flexible beam's vibration.

5.2 Suggestion

In this study, the vibrating shear beam model was controlled by a passivity-based controller. This controller can also be used with other engineering beams, such as Euler-Bernoulli, Rayleigh, and Timoshenko beams. The reason is that since the structure of the proposed controller components consists only of damping and elastic terms, which are the real physical parameters, there is no restriction on their usage in other kinds of beam models.

The possibility of future research may also include the following paragraphs:

In this study, the beam model was investigated without any outside forces or disturbances, so the study of the forced vibration with some disturbance is very interesting. The results of the study can be applied to a wider range of applications.

The investigation of the observer's design parameter, which can be tuned to determine the observer's settling time or the rate at which the observer's response catches up with the full-state controller.

REFERENCES

Boonkumkrong, N., Chinvorarat, S., & Asadamongkon, P. (2018). *Backstepping boundary control: an application to the suppression of flexible beam vibration.* Paper presented at the IOP Conference Series: Materials Science and Engineering.

Boonkumkrong, N., Chinvorarat, S., & Asadamongkon, P. (2022). Passivity-based boundary control for vibration suppression of the shear beam *Advances in Mechanical Engineering, 14(11)*, 1-11.

Boonkumkrong, N., Chinvorarat, S., & Asadamongkon, P. (2023). Passivity-based boundary control with the backstepping observer for the vibration suppression of the flexible beam. *Heliyon, 9*(1), 1-16.

Boonkumkrong, N., & Kuntanapreeda, S. (2014). Backstepping boundary control: An application to rod temperature control with Neumann boundary condition. *Journal of Systems and Control Engineering, 228*(5), 295-302.

Fard, M. P. (2002). Passivity Analysis of Nonlinear Euler-Bernoulli Beams. *Modeling, Identification and Control, 23*(4), 239-258.

Ge, S. S., Zhang, S., & He, W. (2011, June 29 - July 01, 2011). *Modeling and Control of an Euler-Bernoulli Beam under UnknownSpatiotemporally Varying Disturbance.* Paper presented at the 2011 American Control Conference, O'Farrell Street, San Francisco, CA, USA.

Guo, B.-Z., & Jin, F. F. (2010). Backstepping approach to the arbitrary decay rate for Euler–Bernoulli beam under boundary feedback *International Journal of Control, 83*(10), 2098–2106.

Han, S. M., Benaroya, H., & Wei, T. (1999). Dynamics of Transversely vibrating beams using four engineering theories *Journal of Sound and Vibration, 225*(5), 935-988.

He, W., Ge, S. S., Hang, C. C., & Hong, K.-S. (2010, December 15-17, 2010). *Boundary control of a vibrating string under unknown time-varying disturbance.* Paper presented at the the 49th IEEE Conference on Decision and Control, Hilton Atlanta Hotel, Atlanta, GA, USA.

He, W., Sun, C., & Ge, S. S. (2014). Top tension control of a flexible marine riser by using integral-barrier Lyapunov function. *IEEE/ASME Transactions on Mechatronics, 20*(2), 497-505.

He, W., Zhang, S., & Ge, S. S. (2013). Boundary control of a flexible riser with the application to marine installation. *IEEE Transactions on Industrial Electronics, 60(12)*, 5802-5810.

He, W., Zhang, S., & Ge, S. S. (2014). Adaptive boundary control of a nonlinear flexible string system. *IEEE Transactions on Control Systems Technology, 22(3)*, 1088-1093.

Jiu, W. (2003). Boundary feedback stabilization of an unstable heat equation. *Journal on Control and Optimization, 42(3)*, 1033-1043.

Khalil, H. K. (2002). *Nonlinear Systems* (Third ed.). Upper Saddle River, New Jersey: Prentice-Hall.

Kim, J. U., & Renardy, Y. (1987). Boundary control of the Timoshenko beam. *Journal on Control and Optimization, 25(6)*, 1417-1429.

Krener, A. J., & Kang, W. (2003). Locally convergent nonlinear observers. *Journal on Control and Optimization, 42(1)*, 155-177.

Krstic, M., Balogh, A., & Smyshlyaev, A. (2006a, July 24 - 28, 2006). *Backstepping boundary controller and observer for the undamped shear beam.* Paper presented at the In 17th International Symposium on Mathematical Theory of Networks and Systems, Kyoto, Japan.

Krstic, M., Balogh, A., & Smyshlyaev, A. (2006b, December 13-15, 2006). *Backstepping Boundary Controllers for Tip-Force Induced Flexible Beam Instabilities Arising in AFM.* Paper presented at the the 45th IEEE Conference on Decision & Control, Manchester Grand Hyatt Hotel, San Diego, CA, USA.

Krstic, M., Guo, B.-Z., Balogh, A., & Smyshlyaev, A. (2007, July 11-13, 2007). *Observer Based Boundary Control of an Unstable Wave Equation.* Paper presented at the The 2007 American Control Conference, Marriott Marquis Hotel at Times Square, New York City, USA.

Krstic, M., Guo, B.-Z., Balogh, A., & Smyshlyaev, A. (2008a). Output-feedback stabilization of an unstable wave equation. *Automatica, 44(2008)*, 63-74.

Krstic, M., Guo, B. Z., Balogh, A., & Smyshlyaev, A. (2008b). Control of a tip-force destabilized shear beam by observer-based boundary feedback *Journal of control and optimization 47*(2), 553-574.

Krstic, M., Siranosian, A. A., Balogh, A., & Guo, B. Z. (2007, July 11-13, 2007). *Control of strings and flexible beams by backstepping boundary control.* Paper presented at the the 2007 American Control Conference, Marriott Marquis Hotel at Times Square, New York City, USA.

Krstic, M., Siranosian, A. A., & Smyshlyaev, A. (2006, June). *Backstepping boundary controllers and observers for the slender Timoshenko beam: part I – design.* Paper presented at the Proceedings of the 2006 American Control Conference, Minneapolis, Minesota, USA.

Krstic, M., Siranosian, A. A., Smyshlyaev, A., & Bement, M. (2006, December 13-15, 2006). *Backstepping Boundary Controllers and Observers for the Slender Timoshenko Beam: Part II - Stability and Simulations.* Paper presented at the Proceedings of the 45th IEEE Conference on Decision and Control, Manchester Grand Hyatt Hotel, San Diego, CA, USA.

Krstic, M., & Smyshlyaev, A. (2008). *Boundary Control of PDEs : a course on backstepping designs* (First ed.). Philadelphia: Society for Industrial and Applied Mathematics.

Lasiecka, I. (1995). *Control of Systems governed by Partial Differential Equation* Paper presented at the The proceedings of the 34th Conference on Decision & Control, New Orleans, LA.

Lertphinyovong, J., & Khovidhungij, W. (2008). *Backstepping boundary controllers and observers for the Rayleigh beam* Paper presented at the Proceedings of the 17th World congress, The international federation of automatic control, Seoul Korea.

Liu, J. J., Chen, X., & Wang, J. M. (2016). Sliding mode control to stabilization of a tip-force destabilized shear beam subject to boundary control matched disturbance.

Journal of Dynamical and Control Systems, 22(1), 117-128.

Liu, Y., Chen, X., Wu, Y., Cai, H., & Yokoi, H. (2021). Adaptive Neural Network Control of a
Flexible Spacecraft Subject to Input Nonlinearity and Asymmetric Output
Constraint *IEEE Transactions on Neural network and Learning systems*, 1-9.

Liu, Y., Fu, Y., He, W., & Hui, Q. (2018). Modeling and Observer-Based Vibration Control of
a Flexible Spacecraft with External Disturbances *IEEE Transaction on Industrial
Electronics, 66*(11), 8648–8658.

Liu, Z., Liu, J., & He, W. (2018). Boundary control of an Euler–Bernoulli beam with input
and output restrictions. *Nonlinear Dynamics, 92*, 11.

Luo, Z.-H. (1993). Direct strain feedback control of flexible robot arms: new theoretical and
experimental results. *IEEE Transactions on Automatic Control, 38(11)*, 1610-1622.

Luo, Z.-H., Kitamura, N., & Guo, B.-Z. (1995). Shear Force Feedback Control of Flexible
Robot Arm. *IEEE Transactions on Robotics and Automation, 11*(5), 760–765.

Mathews, J. H., & Fink, K. D. (2004). *Numerical Methods Using MATLAB* (Fourth edition
ed.). Upper Saddle River, New Jersey: Prentice Hall.

Matsuno, F., & Murata, K. (1999). *Passivity and PDS Control of flexible mechanical
systems on the basis of distributed parameter system* Paper presented at the
IEEE International Conference on Systems, Man, and Cybernetics, Tokyo, Japan.

Morgul, O. (1992a). Dynamic boundary control of a Euler-Bernoulli beam. *IEEE
Transactions on Automatic Control, 37(5)*, 639-642.

Morgul, O. (1992b). Dynamic Boundary Control of the Timoshenko Beam. *Automatica,
28*(6), 1255-1260.

Padhi, R., & Ali, S. F. (2009). An account of chronological developments in control of
distributed parameter systems *Annual Reviews in Control, 33*, 59–68.

Rao, S. S. (2011). *Mechanical Vibrations* (Fifth ed.): Prentice-Hall.

Sasaki, M., Shimizu, T., Inoue, Y., & Book, W. J. (2012). Self-tuning vibration control of a
rotational flexible Timoshenko arm using neural networks. *Advances in Acoustics
and Vibration*, 1-7.

Sasaki, M., Ueda, T., Inoue, Y., & Book, W. J. (2012). Passivity-based control of rotational

and translational Timoshenko arms. *Advances in Acoustics and Vibration, 2012*, 1-6.

Smyshlyaev, A., Guo, B.-Z., & Krstic, M. (2009). Arbitrary Decay Rate for Euler-Bernoulli Beam by Backstepping Boundary Feedback *IEEE Transactions on Automatic Control, 54*(5), 1134-1140.

Smyshlyaev, A., Guo, B. Z., & Krstic, M. (2008, December 9-11, 2008). *Boundary controllers for Euler-Bernoulli beam with arbitrary decay rate.* Paper presented at the 47th IEEE Conference on Decision and Control Cancun, Mexico.

Smyshlyaev, A., & Krstic, M. (2004). Closed-form boundary state feedbacks for a class of 1-D partial integro-differential equations. *IEEE Transactions on Automatic Control, 49(12)*, 2185-2202

Smyshlyaev, A., & Krstic, M. (2005). Backstepping observers for a class of parabolic PDEs. *Systems & Control Letters, 54(7)*, 613-625.

Zhao, Z., Liu, Y., & Luo, F. (2018). Boundary Control for a Vibrating String System with Bounded Inputs. *Asian Journal of Control, 20*(1), 323-331.

Zhao, Z., & Liu, Z. (2021). Finite-Time Convergence Disturbance Rejection control for a flexible Timoshenko manipulators. *IEEE/CAA Journal of Automatica Sinica, 8*(1), 157-168.

VITA

NAME	Mr. Nipon Boonkumkrong
DATE OF BIRTH	28 July 1959
PLACE OF BIRTH	Bangkok
INSTITUTIONS ATTENDED	King Mongkut's University of Technology, North Bangkok
HOME ADDRESS	24/29 Moo 5, Soi Watsalak Nua, Tiwanon Road,
	T. Banmai A. Pakkred, Nonthburi 11120